



FRIEDRICH-SCHILLER-
UNIVERSITÄT
JENA



Master thesis

Effects of inorganic nitrogen additions on methane and carbon dioxide production from incubated boreal bog samples

Marianne Böhm

geboren am 02.04.1997 in Rosenheim

Matr. - Nr. 199024

Jena, 20.03.2024

Friedrich-Schiller-Universität Jena
Institut für Geographie

Erstgutachterin: Dr. Karin Potthast
(Friedrich-Schiller-Universität Jena)

Zweitgutachterin: Dr. Claire Treat
(Alfred-Wegener-Institut Potsdam)

Abstract

Boreal peatlands face enhanced organic matter cycling due to accelerated decomposition and ecosystem shifts with progressing climate warming. Together with carbon, nutrients that were previously bound in undecomposed organic matter will increasingly become available to the decomposer microbial communities. As they hold a large fraction of the global soil carbon stocks, how northern wetland carbon pools react to rising temperatures and nutrient status is a relevant but so far unresolved question. This thesis studies the impacts of inorganic N addenda on methane and carbon dioxide release from peat in an anaerobic ex-situ incubation at 4 °C and 20 °C. The samples originate from Siikaneva bog, an ombrotrophic peatland in southern Finland where nitrogen scarcity likely limits the activity of the microbial community.

Results from 190 days of incubation show that N addenda reduced cumulative CO₂ and CH₄ production and changed the trajectory of carbon release. Samples from different positions towards the water table exhibited different patterns of carbon mineralization: Samples from above the water table didn't harbor methanogenic archaea in detectable amounts and consequently didn't produce any methane, while in samples from below the water table, methane release equalled or even surpassed that of carbon dioxide. Methanogenesis, and in consequence, total C release from the methane-producing samples, was extremely responsive to a warmer temperature, but the surface samples were indifferent. Higher temperatures and more ammonium led to a higher fraction of carbon released as methane. An important finding was that most patterns in the data remained unexplained unless oxidation state of the addendum were accounted for. Ammonium generally resulted in a stronger reduction per unit compared to nitrate. Nitrate mainly impacted methanogenesis and the CO₂ release connected to it in the same metabolic system. Nitrogen addenda furthermore impacted the temperature sensitivity of carbon release, and differently depending on the sampled layer: Ammonia dampened the temperature effect in subsurface- but increased it in surface samples. Nitrate only had a significant effect on temperature reactivity in the peat from below the water table, where it attenuated CO₂ but increased CH₄ release with temperature.

These results suggest that viewing decomposition through the lens of nitrogen limitation is not ideal for advancing the understanding of peatland greenhouse gas emissions. Other factors, such as co-limitation by other nutrients, competition of different anaerobic metabolic systems, and potential toxicity of N addenda or accumulating metabolic byproducts may explain the observed decrease in greenhouse gas emissions. The isolated observation of N impacts finally indicated that the peatland carbon sink is not endangered by nitrogen release.

Zusammenfassung

In borealen Mooren wird der fortschreitende Klimawandel durch eine Beschleunigung der Zersetzung und einem Wandel der Ökosysteme den Kreislauf von organischem Material antreiben. Neben Kohlenstoff werden auch Nährstoffe zunehmend aus zuvor kaum zersetzter Organik für Zersetzer verfügbar. Da sie einen großen Teil des globalen Kohlenstoffspeichers in Böden ausmachen, ist die Reaktion von Mooren der höheren Breiten auf steigende Temperaturen und Nährstoffverfügbarkeit eine relevante, aber noch nicht zufriedenstellend gelöste Frage. Diese Masterarbeit möchte dazu beitragen, indem sie die Effekte von Zugaben inorganischen Stickstoffs auf die Produktion von Methan und Kohlenstoffdioxid aus Torf in einer Inkubation unter Sauerstoffausschluss bei 4 °C und 20 °C untersucht. Die Proben stammen aus Siikaneva, einem Hochmoor im südlichen Finnland, in dem mangelnde Stickstoffverfügbarkeit vermutlich die Mikrobengesellschaft einschränkt.

Ergebnisse der 190-tägigen Inkubation zeigen, dass N-Zugaben die kumulative Freisetzung von CH₄ und CO₂ verminderten und den Verlauf der Produktionsraten beeinflussten. Proben von ober- und unterhalb des Wasserstands hatten unterschiedliche Produktionsmuster: Die Oberflächenproben beherbergten keine detektierbaren Zahlen an Methanproduzenten und setzten dementsprechend kein Methan frei, während der tieferliegende Torf ebensoviel oder sogar mehr Kohlenstoff als Methan wie als CO₂ emittierte. Die Methanproduktion, und damit auch die gesamte C-Mineralisierungsquote der methanproduzierenden Proben, reagierte sehr empfindlich auf eine erhöhte Inkubationstemperatur, die Oberflächenproben jedoch kaum. Höhere Temperaturen und mehr Ammonium führten zu einem höheren Anteil von Methan an der freigesetzten Gesamtmenge. Ein wichtiges Ergebnis war außerdem, dass die Muster in den Daten deutlich besser erklärt werden konnten, wenn der Oxidationsstatus des zugegebenen Stickstoffs berücksichtigt wurde. Ammonium führte im Allgemeinen zu einer stärkeren Abnahme der Respiration als Nitrat. Nitrat hinwiederum beeinflusste vor allem die Produktion von Methan bzw. die damit in einem metabolischen System verbundene Produktion von CO₂. Die Stickstoffzusätze beeinflussten weiter-

hin die Empfindlichkeit der Kohlenstoffabgabe gegenüber der Temperatur - und das je nach Schicht unterschiedlich: Ammonium dämpfte den Temperatureffekt in Proben unterhalb der Wasseroberfläche, aber verstärkte ihn in den Oberflächenproben. Nitrat wirkte sich in diesem Kontext nur auf die wassergesättigte Schicht aus und führte dort zu einer verminderten Reaktion von CO_2 , aber einer gesteigerten Reaktion von CH_4 auf Wärme.

Diese Ergebnisse deuten darauf hin, dass der Blickwinkel der Stickstofflimitierung nicht ideal für ein verbessertes Verständnis von Treibhausgasemissionen aus Mooren geeignet ist. Andere Faktoren, wie etwa co-Limitierung durch andere Nährstoffe, Konkurrenz zwischen unterschiedlichen Energiestoffwecheln, und möglicherweise Toxizität der Stickstoffbeigaben selbst oder ihrer Stoffwechselprodukte könnten in Kombination die beobachtete Reduktion der Treibhausgasproduktion erklären.

Zusammengefasst deutet diese isolierte Betrachtung der Effekte von inorganischem Stickstoff darauf hin, dass die Funktion borealer Moore als Kohlenstoffsенke nicht durch Stickstofffreisetzung an sich in Gefahr ist.

Contents

1	Introduction	13
1.1	Background: Carbon and nitrogen cycling in boreal wetlands	14
1.1.1	Peat accumulation and peatland carbon storage	14
1.1.2	Drivers of decomposition and greenhouse gas production	15
1.1.3	Coupling of C and N cycle	17
1.1.4	Vulnerability to and nature of predicted changes	19
1.2	Research objectives and hypotheses	21
2	Data and Methods	23
2.1	Origin of peat samples	23
2.1.1	Siikaneva site description	23
2.1.2	Sample collection	24
2.2	Properties of the peat samples	25
2.2.1	Analysis of physical and chemical soil properties	25
2.2.2	Pore water chemistry	26
2.2.3	Microbial assay	27
2.3	Incubation setup	28
2.3.1	Nitrogen treatments	28
2.3.2	Incubation vial preparation	30
2.4	Greenhouse gas fluxes	31
2.4.1	Headspace sampling procedure and gas chromatography	31
2.4.2	Flux calculations	31
2.4.3	Derived metrics	33
2.4.4	Fitting compartment models for decomposition	34
2.5	Statistical analysis of treatment effects	35
3	Results	36
3.1	Sample properties	36

3.1.1	Chemical and physical properties of soil and pore water	36
3.1.2	Microbial community	37
3.2	Observed greenhouse gas fluxes	38
3.3	Effects of sampled layer	39
3.4	Effects of incubation temperature	42
3.5	Effects of nitrogen treatments	44
3.5.1	Total amount of N added	44
3.5.2	Oxidation state	45
3.5.3	Impact of N treatment on temperature sensitivity	47
3.6	Results of fitting decomposition models	47
4	Discussion	49
4.1	Position relative to the water table and microbial community	49
4.2	Temperature reactivity	50
4.3	Nitrogen addenda	51
4.3.1	NO ₃ as competing terminal e ⁻ -acceptor	52
4.3.2	Toxicity of addenda or intermediate products	54
4.3.3	Carbon use efficiency improved by nitrogen	54
4.3.4	Colimitation	55
4.3.5	Diverging effects of N on the slow and fast C pool	55
4.4	Interactions	56
4.5	Realism and representativeness	56
4.5.1	Sample properties	56
4.5.2	Carbon fluxes	57
4.5.3	Nutrient treatments	58
4.5.4	Transferability to the ecosystem scale	59
5	Conclusion and outlook	61
A	Appendix	76
A.1	GC instrument details	76
A.2	Production time series	77
A.2.1	carbon dioxide concentration in blanks	77
A.2.2	CO ₂ -C per g TOC per day	78
A.2.3	CH ₄ -C per g TOC per day	79
A.3	multiple linear models	80
A.3.1	cumulative CO ₂ -C	80
A.3.2	cumulative CH ₄ -C	81

A.3.3	day of peak CO ₂	81
A.3.4	day of peak CH ₄	82
A.3.5	Q10	83
A.3.6	released % g TOC	83
A.4	visualization of fitted decomposition models	85
A.5	nutrients in tap water and bog	89

List of Figures

1.1	Schematic of the coupled C and nutrient cycles, adapted from Reddy et al. (2023). Processes are shown in white boxes and their in- and output compounds in solid boxes. Transformations that require oxygen are coloured in blue. Anaerobic methane oxidation was excluded for simplicity.	18
2.1	Location of the sample site within Europe (small inset), the Siikaneva mire complex (right) and the patterned bog area (drone image, left). On the orthophoto, the boardwalk towards the eddy covariance tower and other flux measurement equipment is visible as a faint white line. Map sources: Drone imagery by Lion Golde and Tabea Rettelbach; topographic map and hillshade by National Land Survey of Finland; Global vector map by Openstreetmap Contributors.	23
2.2	Setup to extract pore water from peat samples with Rhizons	26
2.3	Overview of the incubation layout (figure partially created with biorender.com)	29
2.4	Examples of incubation vials of peat from above (left) and below the water table (right), and a procedural blank (center).	30
3.1	Gene copy numbers of <i>16s</i> g ⁻¹ fresh weight (upper panel) and of <i>mcrA</i> (bottom left) respectively <i>pmoA</i> (bottom right) relative to <i>16s</i>	37
3.2	Time series of carbon dioxide to methane ratio in samples where methane was produced. Note that the vertical axis is logarithmic.	39

3.3	Development of cumulative carbon production over time in the samples treated with ammonium. Within each panel, colors compare N treatment level to the control. Individual samples' data are shown in transparent points and their means as lines. Solid points with errorbars show means \pm standard errors for each group at three time steps of interest. Points are shifted horizontally for better visualization.	40
3.4	Development of cumulative carbon production over time in the samples treated with nitrate. Within each panel, colors compare N treatment level to the control. Note that the control groups are shared between nitrate and ammonium treatments.	41
3.5	Q_{10} of anaerobic carbon dioxide production (left) and methanogenesis (right) in the N treatment groups; mind the different scales of the vertical axis.	42
3.6	Comparing final proportions of TOC respired between treatment groups. Points with errorbars indicate means with standard deviations. Colors differentiate incubation temperature, the panels between peat depths. . .	44
3.7	Modelled decomposition rates [d^{-1}], exchange ratios and labile fraction for all treatment groups, as well as the square root of mean square residuals ($mg\ C\ gdw^{-1}$). Mean and standard error of cumulative C release on the last day are also provided as a reference. Models that did not converge or were considered unreliable are marked in red. Grey bars give an indication of a cell's value relative to the other values in the same column.	48

Abbreviations

AIC	Akaike information criterion
AWT	above water table (Table 2.1)
BWT	below water table (Table 2.1)
C	Carbon (the element, or compounds containing it)
DNRA	dissimilatory nitrate reduction to ammonia
DOC	dissolved organic carbon
GC (-FID)	gas chromatograph (with flame ionization detector)
gdw	gram dry weight (of sample)
gTOC	gram TOC (of sample)
GHG	greenhouse gas, here: carbon dioxide and methane
N	Nitrogen (the element, or compounds containing it)
P	Phosphorous
TC	total carbon content
TDN	total dissolved nitrogen
TN	total nitrogen content
TOC	total organic carbon
TIC	total inorganic carbon
qPCR	quantitative polymerase chain reaction
WT	water table (peat from water table level, Table 2.1)
ww	wet weight of sample

1. Introduction

High-latitude areas are expected to undergo fundamental ecological changes with progressing environmental change. Rising temperatures, altered precipitation patterns, and shifting seasonality will affect all actors of biogeochemical cycles: plants, microbes, fauna, and abiotic processes (Baird et al., 2009).

In the high latitudes, wetlands are a common ecosystem that covers 3.7 million km² (Hugelius et al., 2020). Due to slowed decomposition processes under cold and water-logged conditions, these ecosystems accumulate an especially high detritus C storage. Additionally, carbon is contained in live plant biomass, microbial biomass, or in dissolved or gaseous form (Reddy et al., 2023, pp. 120–123). In total, northern peatlands store 230 Pg C and 3.4 Pg N within an area of 2 mil. km² that is not affected by permafrost (Hugelius et al., 2020), which corresponds to roughly a tenth of the global soil C stocks of 2 270 Pg C (Jackson et al., 2017).

Transfers between these stocks are carried out primarily by microbial activity: Various phyla of bacteria, archaea and fungi form metabolic chains that deconstruct organic matter into simple low-molecular forms of carbon and nutrients - and ultimately carbon dioxide and methane, major greenhouse gases (GHG) (Dolman, 2019, p. 176). However, these complex, interconnected systems of cycles have only been recently incorporated in models that predict the future of global change that humanity will have to adapt to (Nazaries et al., 2013; H. Zhang et al., 2021).

In the context of climate change mitigation, wetlands' capacity for natural carbon sequestration is gaining interest, but possible enhancement of methane production under elevated temperatures and atmospheric CO₂ concentrations may surpass their carbon sink potential (Van Groenigen et al., 2011). Boreal peatlands currently emit 23.6 - 64.2 Tg CH₄ annually, therefore contributing 4 - 11 % of global annual emissions (Petro et al., 2023; Poulter et al., 2017). Global methane emissions are projected to increase, especially from wetlands, and spin up a positive feedback loop with climate change (Dean et al., 2018).

With enhanced decomposition, not only carbon but also nutrients such as nitrogen will

be released from organic matter storages in wetlands (Salmon et al., 2016). Remote effects of industrial fertilization as well as increased litter input from spreading vascular plants are added on top of that (Fowler et al., 2013; Petro et al., 2023). N influences the climate directly as N_2O , but also indirectly by interacting with the C cycle (Dolman, 2019, pp. 176–178). As carbon and nitrogen cycles are tightly linked, and peatlands are typically N-limited, effects of increased N availability on greenhouse gas production can be expected.

Therefore, how wetland greenhouse gas production responds to N availability needs to be studied to improve the understanding of global change and ultimately, to keep global temperatures within a human-friendly range.

This thesis will approach this topic by analyzing an experiment in which CO_2 and CH_4 production were observed in anaerobically incubated samples from Siikaneva bog, an ombrotrophic peatland in boreal Finland, after amending them with varying levels of ammonium and nitrate.

1.1 Background: Carbon and nitrogen cycling in boreal wetlands

1.1.1 Peat accumulation and peatland carbon storage

Peatlands accumulate soil organic matter because their net primary productivity exceeds decomposition rates (Bragazza et al., 2009, p. 99). They have provided a consistent carbon sink throughout the Holocene (Yu, 2011) mainly because decomposition rates are restricted. Glaser and Chanton (2009, pp. 145–146) explain the mechanics as follows:

"Peat accumulation is driven by a high water table, which restricts the zone of rapid decomposition to a thin veneer of organic soil directly above the fluctuating water table. Rates of decomposition decline dramatically below the water table where anoxic conditions prevail and the breakdown of organic matter is restricted to the less thermodynamically efficient processes of fermentation and methanogenesis. The biodegradation of organic matter within this deeper anoxic zone may be further reduced by the increasing fraction organic matter resistant to decay, low temperatures, limited of supply of nutrients, and the accumulation of toxic metabolites. "

Processes on both the in- and output side of this carbon balance are predicted to speed

up with climate change: More CO₂ and CH₄ production are expected for northern peatlands; complementing this, CH₄ oxidation and CO₂ uptake by growing plant biomass will also increase (GCTE-NEWS et al., 2001, Yu et al., 2009, p. 55, Belyea, 2009, p. 15). This study focuses the output side by observing decomposition while excluding primary productivity.

1.1.2 Drivers of decomposition and greenhouse gas production

Decomposition complements net primary production and thus closes the carbon and nutrient cycle. Litter and other compounds released by plants, such as root exudates, provide complex plant polymers that are subsequently broken up into oligomers via extracellular enzyme hydrolysis. These act as substrate for other microbes, providing energy and material for biomass growth.

Ultimately, decomposition produces two carbon compounds - methane and carbon dioxide - that act as greenhouse gases upon entering the atmosphere. In which ratio they are released varies widely in the literature, and depends on the contribution of aerobic and anaerobic degradation processes, which are governed by the position of the water table and the presence of relevant microorganisms. (Nilsson and Öquist, 2009, p. 134).

Boreal bogs are typically moderate sinks of CO₂ and small sources of CH₄ (Alekseychik et al., 2021), but climate projections predict a weakening sink strength (Wu and Roulet, 2014). Methane is the more potent greenhouse gas (Neubauer and Megonigal, 2015) and staying within the remaining global carbon budget depends on the reduction of non-CO₂ emissions (Rogelj and Lamboll, 2024). Peatlands are the largest natural methane source in the northern hemisphere, but large uncertainties still envelope the global budget (Yu et al., 2009, p. 55). For these reasons, this study will put a focus on drivers of anoxic decomposition and methane production in peat samples.

The rate and pathways of organic matter decomposition are determined by a network of factors: substrate quality and quantity, the microbial community, soil aeration status, temperature, and type and availability of alternative electron acceptors. The following paragraphs will shortly introduce each of these factors.

Soil organic matter quality and quantity The quality of organic matter determines how well the substrate can supply a microbial population. It consists of multiple chemical and physical characteristics, whereof no single one can define quality alone, but lignin and nitrogen content are candidates as "key indicators" (Reddy et al., 2023, p. 167). Sphagnum moss, the architect species of bogs, produces litter that is rich in

inhibitory compounds but poor in nutrients, and thus typically decomposes slowly (Bragazza et al., 2009). While nutrients may be abundant in absolute terms, the C:N ratio is unfavourably high, and microbes need to obtain nutrients from their environment in addition to their substrate. With little supply of other organic matter, nutrient availability potentially limits microbial and plant growth, especially in ombrotrophic (rain-fed) peatlands (Reddy et al., 2023).

During decomposition, the C:N ratio typically tightens, as carbon transitions to the atmosphere as carbon dioxide or methane, while N is immobilized in microbial biomass (Amelung et al., 2018, p. 83). Therefore C and C:N typically decrease, while N increases, along peat profiles with depth (Griffiths and Sebestyen, 2016).

Soil aeration status and microbial community Microbial biomass adapts dynamically to its environment (Reddy et al., 2023, p. 171). Wetland microbes are stratified vertically according to oxygen and alternative electron acceptors' presence: aerobic bacteria and fungi thrive above the water table, and facultative or obligate anaerobes populate deeper strata where oxygen is depleted. Therefore, the position of the water table is one central driver of peatland carbon dynamics. Decomposition under oxic conditions, being more energetically favourable, achieves 2-3 times more mass loss (Bragazza et al., 2009, p. 102).

Aerobic respiration results in the complete decomposition of organic matter to carbon dioxide. In the absence of oxygen, respiration depends on alternative terminal electron acceptors (see below) and a complex metabolic network of microbes that performs a chain of "chemical handoffs" (Dolman, 2019, p. 176), including hydrolyzation and fermentation, where products of one step provide substrate for the next.

Ultimately, methane is produced by archaea of the phylum *Euryarchaeota*. Three main methanogenic pathways - hydrogenotrophic, acetoclastic and methylotrophic - allow them to utilize different substrates: CO₂, acetate, and methyl group containing compounds such as methanol and methylated amines (Nazaries et al., 2013). In ombrotrophic peatlands, hydrogenotrophic methanogenesis dominates (Artz, 2009, pp. 112–16).

The complexity of the anaerobic respiration system brings about that it reacts sensitively to disturbance (Nilsson and Öquist, 2009, p. 141). Methanogens in particular are sensitive to environmental conditions like temperature and pH, but their competitive and adaptive strategies are poorly known (Bodelier and Steenbergh, 2014; Nazaries et al., 2013).

Most methane is oxidized to carbon dioxide on its way upwards through the oxic zone

(Dean et al., 2018). Additionally, anoxic methane oxidation pathways that rely on a coupled energy pathway have also been discovered and may be widespread (Gupta et al., 2013; Raghoebarsing et al., 2005).

Availability of electron acceptors ("redox ladder"): Where oxygen is unavailable, other compounds are used as electron acceptors to facilitate organic matter oxidation. Depending on their redox potential, a sequence of alternative e^- - acceptors are used under increasingly reducing conditions and with decreasing energy yield: 1. nitrate, 2. manganese, 3. ferric ions, 4. sulfate and 5. carbon dioxide (hydrogenotrophic methanogenesis), among others. Decomposition of organic matter supported by the most favourable compounds is carried out by facultative anaerobes and works similarly to oxic conditions, in that it produces mainly carbon dioxide and the reduced form of the oxidant. Once competing terminal e^- - acceptors are depleted, methanogenic conditions are reached (Amelung et al., 2018; Nilsson and Öquist, 2009; Reddy et al., 2023).

Temperature influences many bio-chemical processes in decomposition, such as enzymatic activity and the survival and growth of cells. In general, they are boosted in warmer conditions until a specific optimum is crossed. The reaction of net carbon flux of an ecosystem to temperature changes integrates different sensitivities of the involved processes. Heterotrophic respiration is mainly controlled by temperature, and more so than primary productivity (Rankin et al., 2022). Reactions with less favourable energy outcomes tend to be more temperature sensitive, for example the decomposition of low quality material or methanogenesis (Reddy et al., 2023).

1.1.3 Coupling of C and N cycle

The carbon and nitrogen cycles are tightly linked, as all organisms require both elements in their biomass, and both are released together when organic matter is broken down. Additionally, some anaerobic decomposition pathways involve a connection to N transformations. Figure 1.1 gives an overview of the coupled C and N cycles.

N in wetlands can exist as inorganic compounds such as N_2 , NH_4^+ , NO_2^- , NO_3^- , NO, and N_2O . Organic forms include proteins, nucleic acids and amino sugars (Reddy et al., 2023) and are usually more abundant than inorganic forms (Weedon et al., 2012). Of all these, ammonium, nitrate and amino acids make up the plant-available N forms. Microbes acquire (immobilize) N via biological N fixation (BNF) or assimilation of nitrate or ammonium. While nitrate is soluble and easily leached, ammonium is more stable and often adsorbed to clay minerals (Amelung et al., 2018, p. 523). Nitrate fur-

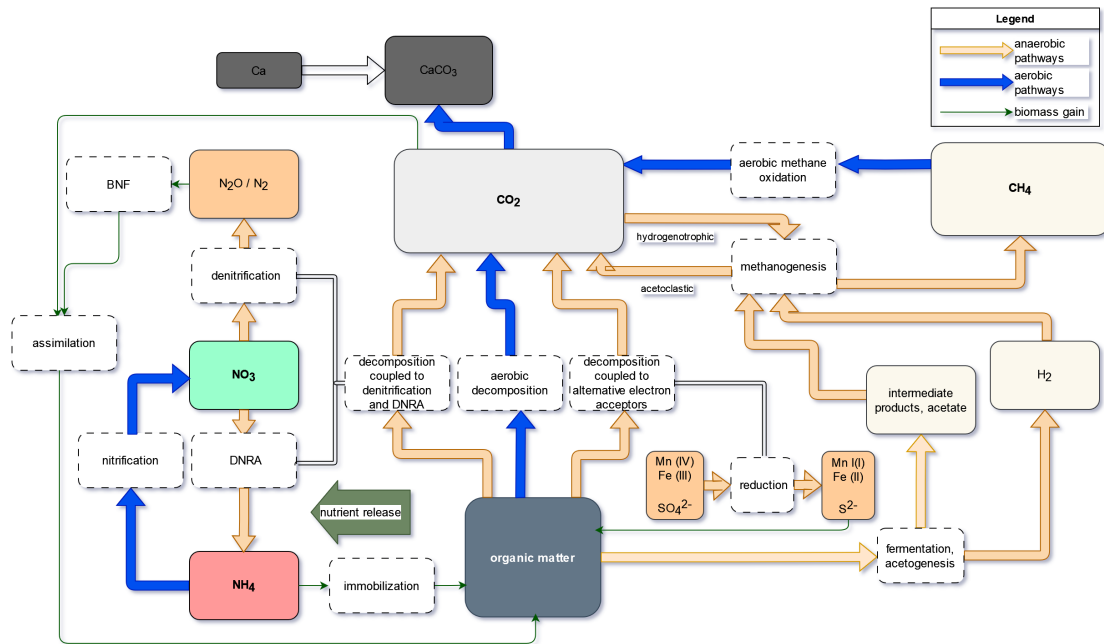


Figure 1.1: Schematic of the coupled C and nutrient cycles, adapted from Reddy et al. (2023). Processes are shown in white boxes and their in- and output compounds in solid boxes. Transformations that require oxygen are coloured in blue. Anaerobic methane oxidation was excluded for simplicity.

Furthermore, nitrate is transformed to gaseous N₂ or N₂O (denitrification) or reduced to ammonia, and serves as a terminal electron acceptor in the associated decomposition pathways. Ammonium may be transformed back to nitrate via nitrification, but only under oxygen supply. Consequently, it accumulates in the anoxic zone, while nitrate forms near the surface and migrates downwards (Reddy et al., 2023, p. 353). Therefore, ammonium concentrations increase with depth (Griffiths and Sebestyen, 2016).

The fundamental coupling of the two cycles expresses itself in a sensitivity of decomposition towards nutrient status, for example in incubations: Second only to carbon content, N content strongly controls how much carbon gets mineralized (Knoblauch et al., 2013). N addenda are incorporated into additional microbial biomass, and stimulate the decomposition of labile carbon, but attenuate complex carbon deconstruction (Lavoie et al., 2011; Currey et al., 2009). Furthermore, soil nutrient status seems to steer the temperature response of respiration (Weedon et al., 2013; H. Zhang et al., 2021).

Methanogens need to acquire N like any other organism and can be N-limited. At the same time, some N compounds may inhibit methanogenesis, either as oxidant (NO₃, NO₂) for denitrifiers that outcompete methanogens for substrate, or as the basis for den-

nitrification whose intermediate products (NO_2 , N_2O and NO) are toxic to methanogens (Bodelier and Steenbergh, 2014).

The terrestrial N cycle is heavily modified by human activity, particularly by the Haber-Bosch process, the chemical process to produce industrial fertilizer (Dolman, 2019, p. 181). This has led to an enrichment of the biosphere with N relative to C and fueled the additional yearly uptake of 2.6 Pg terrestrial C (Zaehle, 2013).

1.1.4 Vulnerability to and nature of predicted changes

Müller and Joos (2021) estimate that under the boundary conditions of 2014, 10% of northern peatland carbon until 2100 will be lost, mainly through a decline in peatland area. Even higher losses are expected in climate scenarios with higher radiative forcing, but a notable amount is also preserved in relict peat horizons after the transition to different ecosystems. Local precipitation and temperature were the main drivers of area changes. These results suggest that large parts of today's northern peatlands might be at risk under future climate change - and the high latitudes are warming even faster than the global average (Intergovernmental Panel On Climate Change, 2023). In peatlands, temperature increases lead to faster N cycling, due to enhanced decomposition but also ecosystem shifts that go along with the expansion of vascular plants that shed more leaf and root litter (Weedon et al., 2012; Iversen et al., 2023). In reverse, external N supply determines whether climate warming promotes vascular plants (high N) or sphagnum growth (low N), tipping the balance between net C release or accumulation (Heijmans et al., 2008).

Nutrient inputs into ombrotrophic peatlands are suspected to be influential because these ecosystems are typically nutrient-limited. Firstly, by definition, they receive little external input - only atmospheric gaseous or particulate sources or precipitation, but no lateral inflow. Any present nutrients are severely competed for and quickly immobilized (K. Dierßen and B. Dierßen, 2001, p. 66).

Previous studies found significant impacts of N, either as artificial additions or along natural gradients, on carbon dynamics in peatlands. Bragazza et al. (2006) observed increased CO_2 and DOC release along a gradient of increasing atmospheric N deposition across European bogs, and conclude that removing microbial N limitation and improving litter quality will endanger the C sink that bogs currently provide. Similarly, field studies found that inorganic N additions generally intensified CH_4 emissions and reduced its uptake (Liu and Greaver, 2009; Nazaries et al., 2013). A recent review (Bobink et al., 2022) outlines that both stimulating or neutral responses of greenhouse gas production to N amendments have previously been found.

While the fact that nitrogen impacts the carbon cycle somehow is quite established, the implications of this connection on the net carbon release or uptake of ecosystems are less clear and driven by several interacting factors. For example, nutrient availability reinforces how strongly methanogenesis reacts to temperature changes (H. Zhang et al., 2021). Additionally, the trend direction may vary depending on the recalcitrance of the substrate: while labile carbon pools are depleted more quickly in N-amended peat, the less easily available carbon sources are utilized to a lesser extent in some studies, and effects varied over time (Currey et al., 2009; Lavoie et al., 2011). Finally, Currey et al. (2009) also found contrasting effects of N supplied as nitrate or ammonia: while nitrate had no significant effects, respiration rates were lowered by small and enhanced by large amounts of additional ammonia.

To conclude, boreal bogs' responses to nutrient status and warming have been observed in several large-scale studies, like in the Whim Moss in Scotland (Sheppard et al., 2013) and the SPRUCE experiment in Minnesota, US (Petro et al., 2023). However, there is a lack in small-scale studies like incubations that allow more control of environmental parameters and therefore better insights into the effects of nitrogen additions on methanogenesis, which are still "controversial" (Nazaries et al., 2013).

N sources in wetlands

The following paragraphs will provide an overview of nitrogen sources and their scales in peatlands: namely atmospheric deposition, biologic nitrogen fixation and decomposition of organic matter.

Firstly, nitrogen can enter terrestrial ecosystems via deposition from the atmosphere. Ammonia and nitrate, originating for example from agricultural fertilizer dust, are transported bound to aerosols (Dolman, 2019, p. 180). Deposition increased during the years of 1850 - 2000, including in southern Finland (Artz, 2009, p. 111, Dolman, 2019, p. 185,). Southern Finland receives 200-400 mg N m⁻² yearly from atmospheric deposition in equal parts in oxidized and form (model results for 2021, EMEP, 2023). This is below the critical threshold for bogs at 500-1000 mg N m⁻² (Bobbink et al., 2022), but enough to place Siikaneva within the risk areas for both eutrophication and biodiversity loss in 2020 (Hettelingh et al., 2017, p. 15). Additionally, damages may occur at the lower end of this threshold already, and lower thresholds have been proposed for similar ecosystems (e.g. Wieder et al., 2019).

N-associated risk projections have been moderated between 2005 and 2020 (Hettelingh et al., 2017). The nearest available observations at Valkea-Kotinen observed a small decrease of total inorganic nitrogen deposition over 1990-2012 (Vuorenmaa et al., 2017).

Furthermore, some microbes that are addressed collectively as diazotrophs fixate molecular nitrogen. They are taxonomically placed within the *Cyanobacteria* and *Actinomyces*. Some live symbiotically with sphagnum mosses, are anaerobes, and/or methanogens or sulfate reducers. Inorganic N addition suppresses their activity (DeLaune et al., 2013) as well as warming, likely through competition with less energy-intensive N sources (Petro et al., 2023). Biologic nitrogen fixation contributes a notable N influx on the order of 36.5 - 2190 mg N m⁻² yr⁻¹ in peat bogs (DeLaune et al., 2013, pp. 287–90).

Finally, N travels along the cycle of growth and decomposition within the peatland. Immobilization binds around 65 kg N ha⁻¹yr⁻¹ (K. Dierßen and B. Dierßen, 2001, p. 143). Climate warming is projected to increase nutrient release within wetland ecosystems by enhancing decomposition. For example, Iversen et al. (2023) show that with (artificially) elevated temperatures in a live bog ecosystem, available ammonia and phosphate rise exponentially, and without any mitigation by heightened CO₂ concentrations. Similarly, simulated climate change (warmer summers) led to accumulation of organic N plus both ammonia and nitrate in Weedon et al. (2012). This is partly related to sphagnum mortality as the ecosystem shifts with stronger warming and brown mosses and higher plants outcompete sphagnum (Bragazza et al., 2009; Petro et al., 2023, p. 104). Enhanced decomposition thus works through three processes: accelerated decomposition of existing organic matter, temporary influx of dead plant material, and sustained amplification of litter input from higher plants.

1.2 Research objectives and hypotheses

This thesis aims to answer the main research question “**What effect do increased levels of ammonia and nitrate have on CO₂ and CH₄ production from Siikaneva bog?**”, namely on the total amount of C respired as either gas, the ratio between them, and their development in time. Additionally, it will investigate how this effect depends on the form of nitrogen (oxidized or reduced), and how these factors interact with temperature and source layer.

Based on the existing research outlined in chapter 1, the following hypotheses describe the expected results that will be compared to this study’s new data:

1. According to basic biological principles, **higher respiration rates are expected in warmer temperatures.**
2. **A time lag until the beginning of methane production is expected in the surface**

layer samples, as the microbial community needs to adapt to anoxic conditions first, while the below-water-table community thrives under conditions closer to their natural environment.

3. Both inorganic N forms are easily available nutrients that microbes can assimilate. Increased supply should facilitate microbial growth and their capability to decompose organic matter. **Thus higher additions are proposed to lead to higher respiration.**
4. Supplying N in oxidized or reduced form is expected to lead to different effects.
 - (a) **Nitrate addition specifically should stimulate decomposition.** Nitrate is vital to decomposition processes in anoxic conditions, being the second-most energetically favourable electron acceptor after oxygen. Additionally, NH_4^+ is accumulating under anoxic conditions, while NO_3^- is depleted - and more generally, wetlands are typically limited in electron acceptors, but not -donors (Reddy et al., 2023, pp. 174–175). Consequently, adding nitrate is expected to be more influential than ammonium.
 - (b) **$\text{CO}_2:\text{CH}_4$ is increased by availability of terminal e^- acceptors like NO_3^-** (Artz, 2009, p. 137), so this should be mirrored in this experiment, at least initially.
5. **Nitrogen addenda are expected to intensify the decomposition of labile carbon, but not of recalcitrant substrate.**

2. Data and Methods

2.1 Origin of peat samples

2.1.1 Siikaneva site description

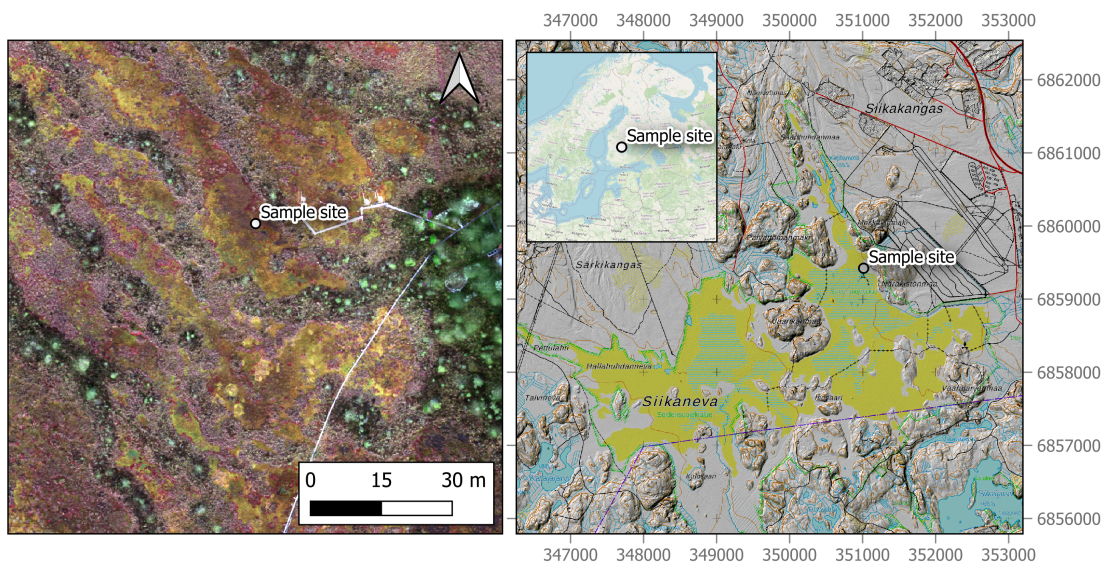


Figure 2.1: Location of the sample site within Europe (small inset), the Siikaneva mire complex (right) and the patterned bog area (drone image, left). On the orthophoto, the boardwalk towards the eddy covariance tower and other flux measurement equipment is visible as a faint white line. Map sources: Drone imagery by Lion Golde and Tabea Rettelbach; topographic map and hillshade by National Land Survey of Finland; Global vector map by Openstreetmap Contributors.

The peat samples used in this study originate from the Siikaneva peatland complex in Ruovesi, western Finland; the exact location is indicated in Figure 2.1. In peat cores,

Mathijssen et al. (2016) found ages up to 11 000 years and peat depths between 2.4 and 6.8 m. They estimate a current carbon storage of almost 1000 Gg C.

Mean annual rainfall in Siikaneva amounts to 711 mm (Alekseychik et al., 2021) The Juupajoki-Hyytiälä weather station some 10 km from the site records an average annual temperature is 4.2 °C, with -7.2 °C in January and 17.1 °C in July (averages of the 30-year period 1982–2011, Korrensalo et al., 2018). Most years between 2011 and 2016 had warmer and drier summers than the 30-year average (Alekseychik et al., 2021). In 2022, mean air temperatures were at 16.3°C in summer and 6.7°C in autumn, and soil temperatures at 2 cm depth were similar with a slightly buffered variability (Jentzsch et al., 2024, *in review*).

Siikaneva hosts several research projects and infrastructure (e.g. Baysinger et al., 2024, Korrensalo et al., 2018, Jentzsch et al., 2024). It features an eddy covariance tower that recorded a net uptake of CO₂ of 61 ± 24 g C /m² and net CH₄ release of 7.1 ± 0.7 g C /m² per year during the growing season of 2011-2016 (Alekseychik et al., 2021).

The Siikaneva complex lies within the southern boreal vegetation zone (Korrensalo et al., 2018). Siikaneva is an open peatland that comprises both ombrotrophic and oligotrophic parts. This study focuses on the ombrotrophic bog area. Within its "mosaic of plant communities", Korrensalo et al. (2018) differentiate seven types of microsites: High Hummock, Hummock, High Lawn, Lawn, Hollow, Bare Peat, and Water. These differ in species composition according to the local distance of the water table from the surface. Sphagnum lawn occupies around 13% of the bog area of Siikaneva (Golde, 2023, *unpublished thesis*), and was sampled for this study. This microform is characterized by a productive moss layer dominated by *Sphagnum papillosum*, *S. magellanicum* and *S. balticum* and hosts few vascular plants. Compared to other microtopographies, it is low in C and N contents and relatively wet: the water table was detected at 4 cm below the moss surface (Korrensalo et al., 2018).

2.1.2 Sample collection

Shallow peat samples were obtained in October 2022 from a homogeneous sphagnum lawn at three locations within several meters distance (see Figure 2.1). Three horizons were distinguished according to the position of the water table. The soil material was cut out in bulk with a bread knife, and transported and stored at 4°C in heat-sealed aluminium bags under dark and anaerobic conditions until the incubation was started in April 2023. The following table (2.1) provides an overview of the sample material.

layer	depth	spatial replicate	analysis
AWT	0 - 3 cm	1	
(above water table)	0 - 3 cm	2	GHG production + geochemical
	0 - 2 cm	3	
WT	3 - 6 cm	1	
(water table)	3 - 7 cm	2	geochemical only
	2 - 6 cm	3	
BWT	6 - 15 cm	1	
(below water table)	7 - 20 cm	2	GHG production + geochemical
	6 - 16 cm	3	

Table 2.1: Overview of the sample material

For the experiment, two depth layers were created by mixing the material from the spatial replicates from similar horizons: the surface layer above the water table (AWT), and the layer that was clearly below the water table (BWT). While intact sphagnum and sedges in colours ranging from vivid green to light brown or red made up the AWT samples, the BWT layer consisted of a medium brown slurry of partly decomposed leaves. Both contained sporadic parts of sedges and other higher plants. Material from the periodically oxic zone was not incubated to prioritize the clearly distinguishable layers above and below.

2.2 Properties of the peat samples

2.2.1 Analysis of physical and chemical soil properties

From the frozen archive portion of the peat moss samples, 30.0 g (AWT) and 55.6 g (BWT) were extracted and placed in plastic bags. These were covered with tissues and dried overnight in a sublimation dryer at 50°C.

Gravimetric water content was determined by comparing the masses of the same sample before and after drying. Once dry, around 1 g of each homogenized sample was ground into a fine powder using a planetary mill with corundum containers at 300 turns per minute. The milling process was run for four minutes initially and then repeated for two minutes until no fibers were visible in the powder.

Powdered samples were analyzed for carbon content in a *elementar soli TOC cube* (Elementar Analysensysteme GmbH, Germany) from two aliquots of each sample. This instrument uses combustion to release all carbon compounds from powdered samples,

uses N_2 to carry it through a Platinum catalyst and filters for moisture and reactive compounds like halogens, and finally detects the produced CO_2 using infrared absorption. A temperature ramp is employed to distinguish between organic carbon (mobilized at $400^\circ C$), residual organic carbon ($600^\circ C$) and inorganic carbon ($900^\circ C$).

Nitrogen contents were measured in a *elementar exceed rapid maxN* (Elementar Analysensysteme GmbH, Germany), which detects total N content by a similar principle as the TOC analyzer described above, but using a constant temperature program and Helium as carrier gas.

2.2.2 Pore water chemistry

Pore water was extracted from subsamples of archived homogenate that were thawed at $4 - 10^\circ C$ in whirlpaks. A Rhizon Soil Moisture Sampler (Rhizosphere Research Products bv, Netherlands; type *MOM*, 10 cm length of porous part, $0.12 - 0.18 \mu m$ pore width) was inserted into each sample, then the packs were wrapped tightly in tape, and a plastic syringe was connected to the Rhizon with an adapter. A vacuum was applied by pulling the plunger and holding it in place with a piece of plywood. The extraction was conducted in a dark storage room at $4^\circ C$. Every few hours, when some water had accumulated and the negative pressure had weakened, the syringes were emptied into a clean Schott glass bottle and re-installed. The extraction was continued until a target amount of 30 ml was retrieved, which took about 24 h. About 1.8 ml of water were transferred into 2 ml Eppendorf tubes and stored frozen, in order to preserve them for nitrate and ammonia analysis which was not possible due to instrument failure at the time of extraction.

Of the tap water that was used to create the treatments, no subsample had been preserved in similar conditions as the peat samples. Thus values measured by the water management office (Energie und Wasser Potsdam GmbH, 2022) are reported in the results.

Electric conductivity and pH Electric conductivity was measured with a probe (WTW TetraCon / Cond340i, Xylem Analytics Inc.). To optimize sample use, a few ml of water sample were filled into a small plastic bag that was wrapped tightly around the probe to ensure its full immersion. The pH was measured by inserting a probe (ThermoScientific Orion VersaStar



Figure 2.2: Setup to extract pore water from peat samples with Rhizons

Pro, Thermo Fisher Scientific) into the small bag that was previously used for EC.

DOC and TDN Dissolved organic carbon and nitrogen are often operationally defined as those C or N containing compounds that pass a certain filter, usually of 0.45 μm pore size. Its sources are standing dead biomass, detritus and soil organic matter from which it is leached or released during decomposition, as well as potential allochthonous entry with water; it then serves as a very mobile pool of carbon and energy within the wetland ecosystem (Reddy et al., 2023, p. 193). In the ombrotrophic Siikaneva bog, inorganic carbon is assumed to be negligible. Relevant organic N components include amino acids that organisms can acquire as nutrients. Inorganic dissolved nitrogen comprises dissolved gases (N_2 , NH_3 , N_2O) and solids like NH_4^+ , NO_2 and NO_3 , but is usually only a small fraction of less than 3% of TDN (Reddy et al., 2023, pp. 286–287). In this study, the observed components must be smaller than the Rhizon membrane size of approximately 0.15 μm pore width. Note also that the results don't purely represent contents of extracellular water that was adsorbed to the sphagnum, but rather, contents of microbial or plant cells that were destroyed when the samples were frozen and thawed are also detected. Furthermore, both dissolved partitions are also included in the solid C and N because it was conducted on water-saturated samples.

20 ml of each sample were decanted into glass exetainers and stabilized by acidification with 25 μL HCl (30% suprapure). Contents of dissolved organic carbon and nitrogen were analyzed in a TOC-L analyzer (Shimadzu, Japan) extended with a TNM-1 module by combustion catalytic oxidation: the liquid sample is heated to 720°C in the presence of a platinum catalyst and oxygen supply. The resulting CO_2 and N_2 are quantified using an infrared gas analyzer and a chemoluminescence detector, respectively. TOC is reported as NPOC (non-purgeable organic carbon).

Bulk density measurements had not been taken from the unaltered samples before they were placed in bags. Therefore, to approximate, existing data obtained in 2021 from the same site were selected for the appropriate depths and averaged (Johanna Schwarzer, unpublished data).

2.2.3 Microbial assay

Quantitative Polymerase Chain Reaction (qPCR) was used to quantify three key genes of microbial methane cycling: *mcrA*, a subunit of the gene encoding methyl coenzyme M reductase - an enzyme common to all methanogenic pathways - indicates the abundance of methanogens; *pmoA* 621-R/ *pmoA* mb661-R (particulate methane mono-

oxygenase) is related to methane oxidizers; and *16s* serves as a marker of total bacterial abundance (Nazaries et al., 2013; Peltoniemi et al., 2016). Samples were processed as in Laurent et al. (2023) in technical triplicates from multiple subsamples, which were taken from the homogenized peat during the incubation setup in the anaerobic workstation. Copy numbers of *mcrA* and *pmoA* were put in relation to *16s* to gauge their relative importance in the microbial community (note that methane cycling is conducted by archaea, which are not represented in the *16s* result).

2.3 Incubation setup

To study process rates of organic matter decomposition and how they are impacted by variations in environmental factors, incubations are a common tool that allows the researcher to tightly control the factors of interest. In an incubation vial, complex interactions of real ecosystems are simplified, and any outputs can be monitored (Schädel et al., 2020).

In this study, a laboratory incubation of peat material under anoxic conditions was conducted in order to monitor changes in GHG production under a factorial variation of N addition. By design, this setup excludes any transport processes of substrate, nutrients, and gases in and out of the observed material, other than through gas exchanges with the headspace. The peat was incubated at two temperatures: a) at 4 °C to represent shoulder-season conditions, which contribute a non-negligible fraction of yearly emissions in northern ecosystems b) at 20 °C to simulate maximum potential production during a very warm summer (climate data see Alekseychik et al. (2021)). A nitrogen-gas headspace and water additions simulated completely waterlogged, anoxic conditions. We assume that due to the lack of oxygen, no methane was oxidized, and fungal decomposition can be neglected.

Figure 2.3 presents the concept of the incubation experiment.

2.3.1 Nitrogen treatments

Baseline contents of Nitrogen species were estimated using a measurement of Total Dissolved Nitrogen (TDN) and literature values of typical fractions of ammonium and nitrate: TDN in porewater was measured in situ at several sites and depths in October 2022 (Jentsch et al., 2024, *in review*). For this experiment, the results from the appropriate microtopography (hollow) at 7 cm and 20 cm depth were averaged to yield a mean concentration of 0.495 mg l⁻¹. Contents of nitrate and ammonia in leachate as reported by Treat et al. (2016) for their control group in the fall season were applied to estimate

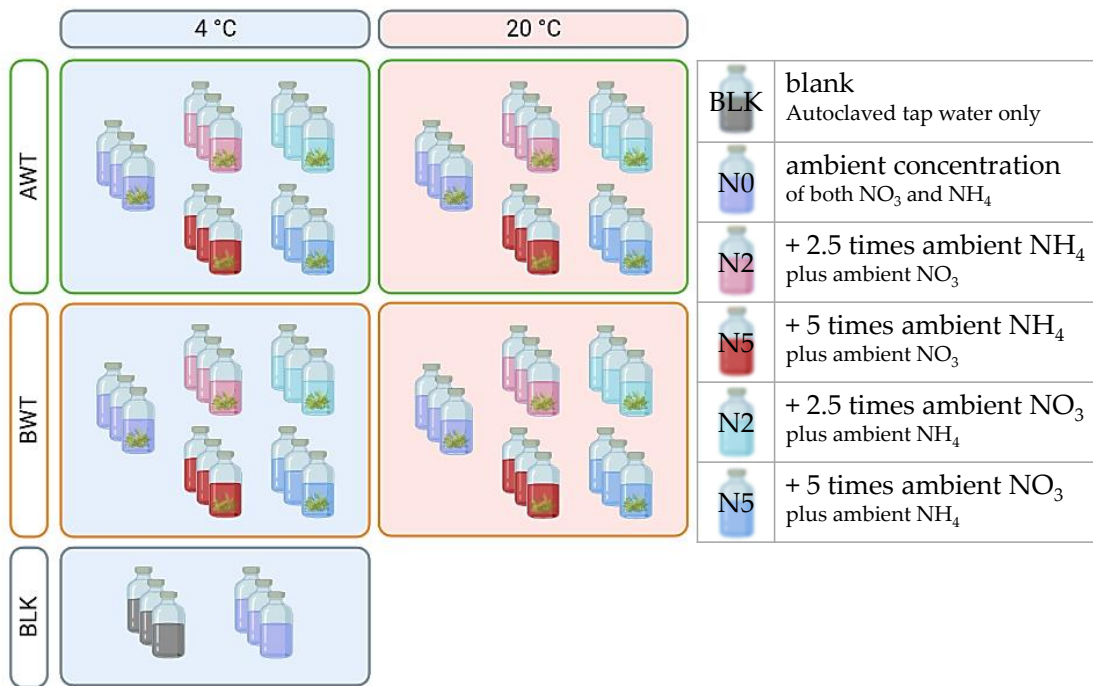


Figure 2.3: Overview of the incubation layout (figure partially created with biorender.com)

the target concentrations. The applied ratios were: $\text{NH}_4 : \text{TDN} = 0.19$, $\text{NO}_3 : \text{TDN} = 0.61$, resulting in the target concentrations listed in table 2.2.

treatment		total N mg l^{-1}	$\text{NH}_4\text{-N}$ mg l^{-1}	$\text{NO}_3\text{-N}$ mg l^{-1}
N0	ambient	0.495	0.094 1	0.302
N2	+ 2.5 x ambient	1.73	0.329	1.06
N5	+ 5 x ambient	2.97	0.565	1.81

Table 2.2: Target concentrations of total dissolved nitrogen, ammonium and nitrate

To create the nitrogen treatments, either ammonium chloride (NH_4Cl) or sodium nitrate (NaNO_3) were added to autoclaved tap water. The concentrations of the stock solutions were calculated so as to preserve ambient concentrations (2.2) for the N0 group, and to add 2.5 times or 5 times ambient concentrations for the N2 and N5 treatment groups, respectively, while also accounting for the molecular weight fraction of nitrogen in either salt and the high natural water content of the samples (assumed to be 95%).

treatment group	NH ₄ Cl mg L ⁻¹	NaNO ₃ mg L ⁻¹	NH ₄ -N μg	NO ₃ -N μg	total N μg
CTR-N0	3.56	18.4	0.941	3.02	3.96
NH4-N2	20.9	18.4	5.53	3.02	8.55
NH4-N5	38.3	18.4	10.1	3.02	13.1
NO3-N2	3.56	107	0.941	17.8	18.7
NO3-N5	3.56	197	0.941	32.5	33.4

Table 2.3: Concentrations of ammonia and nitrate solutions used for Nitrogen treatment and resulting amounts of N, in either form or in total, added to each vial.

2.3.2 Incubation vial preparation

For each layer separately, the bags were opened inside an anaerobic workspace, emptied into a large beaker together, and mixed thoroughly using sterilized lab equipment. The three cores contributed evenly to the pool replicate. 10g of this mix were weighed into 120 ml glass incubation vials. Large twigs or roots were removed to avoid in-homogeneous distributions of materials in the incubation vials. All leftovers were stored in a freezer at -25 °C for further analysis and archive purposes.



Figure 2.4: Examples of incubation vials of peat from above (left) and below the water table (right), and a procedural blank (center).

For the N treatments, 1 ml of the designated stock solution was added to each incubation vial along with 1 ml N0 solution of the other nitrogen species (Table 2.3) and 8 ml autoclaved tap water to achieve a total addition of 10 ml H₂O. The vials were then sealed with rubber stoppers, secured with aluminum crimps, and flushed with N₂ for 5 minutes (see Figure 2.4). After taking the first headspace sample, the incubation vials were stored in dark incubators with constant temperatures of 4°C or 20°C according to their treatment group.

2.4 Greenhouse gas fluxes

2.4.1 Headspace sampling procedure and gas chromatography

To determine greenhouse gas concentrations, the incubation vial headspaces were sampled regularly with a syringe. Multiple samples were taken during the first week, then the sampling interval was relaxed to weekly and then monthly as productivity declined. Vials were gently shaken before the procedure to release any trapped air bubbles and enforce equilibration between the water and the gas phase. One sampling sequence consisted of extracting 5.5 ml of headspace gas through the stopper with a sterile needle, flushing 0.5 ml and injecting 5 ml into an evacuated 20 ml exetainer with a rubber septum. The incubation vials were then repressurized by injecting 5.5ml N₂. The sample exetainers were run through a Shimadzu Nexis GC-2030 gas chromatograph equipped with an automated headspace sampler (Shimadzu, Japan). CO₂ and CH₄ concentrations were determined by a flame ionization detector (GC-FID) with a Jetanizer component for detecting CO₂ (More details on the instrument's internals are given in the appendix A.1). As instrumental blanks, evacuated vials were run alongside the samples. Gas concentrations were computed from the chromatogram peak areas via a calibration curve. Over the course of the experiment, the retention time of CO₂ moved from 12.59 to 12.98 minutes. A new calibration was conducted in July 2023 and applied to all data.

Whenever a threshold of 10 000 ppm of either gas was crossed, the vial was flushed with N₂ for 3 minutes on the subsequent measurement date, and measured again to obtain a baseline concentration. By this procedure, concentrations in the headspace are kept within a natural range (e.g. < 14 000 ppm CH₄ in H. Zhang et al., 2021; see also Laurent et al., 2023; Knoblauch et al., 2013), as excessively high headspace concentrations would inhibit further production (Nilsson and Öquist, 2009).

2.4.2 Flux calculations

Quality control

Data quality was ensured by the following measures:

- taking notes of mistakes such as erroneous amounts of gas sample,
- analyzing chromatograms by eye to find any abnormalities,
- plotting the time series of concentrations and production rates of all replicates of each treatment group, identifying any unrealistic outliers, and

- compiling this knowledge in a flag column, indicating if a sample was reliable (0), suspicious (1) or totally unreliable (2). Data points assigned to the last category were excluded and treated as if no data had been obtained. Group 1 data were included, but subjected to additional checks and discarded if necessary.

Concentrations in procedural and GC blanks were plotted to identify any issues with the measurement procedure. One set of measurements had to be discarded entirely due to instrument failure.

Production rates of CH₄ and CO₂

All data analyses were carried out in R (version 4.3.1) within the RStudio programming environment and relied mainly on packages within the "tidyverse" for data management (R Core Team, 2023; Wickham et al., 2019). Microsoft Excel was used to digitize lab notes and to manually compile and edit tabular data.

To prepare for analysis, the calibrated GC outputs from all dates were collected in one file along with quality annotations. Any negative concentrations - that arise from the calibration curve not being forced to cross the origin - were set to zero, and necessary information on the samples was attached.

To account for the dilution of gas concentrations caused by the sampling procedure, a post-sample concentration was calculated for each date using the formula $d = (vol_h - vol_x) / vol_h$, wherein the dilution factor d is calculated from the headspace volume vol_h and the volume of exchanged gas vol_x . For this step, headspace volume was estimated using moss bulk density (3.1) and known weights. Pressures were assumed to be constantly at 1 atm for the calculations.

The concentrations were then converted to $\mu\text{g C}$ per vial applying the ideal gas law:

$$C_m[\mu\text{g/L}] = \frac{C_v[\text{ppm}] * M[\text{g/mol}] * P[\text{atm}]}{R[\frac{\text{L*atm}}{\text{K*mol}}] * T[\text{K}]}$$

with

C_m : concentration in mass per volume

C_v : concentration expressed as amount fraction

M : molar mass of carbon

P : pressure

R : universal gas constant in the appropriate unit

T : temperature

(Robertson et al., 1999). Proportionally to the headspace concentration, a fraction of the gases dissolves into the water contained in the incubation vial. The relation between concentrations of the gaseous and aqueous phase at equilibrium is quantified by the Henry's law constant for a given gas and temperature. After Burkholder et al. (2019), the constants applied here are:

$$H_s(\text{CO}_2) = 3.44 * 10^{-2} \frac{M}{atm} \text{ and}$$

$$H_s(\text{CH}_4) = 1.41 * 10^{-3} \frac{M}{atm}$$

(transformed to concentration/concentration basis using the online tool provided by Sander (2023) to $H_{cc}(\text{CO}_2) = 0.842$, $H_{cc}(\text{CH}_4) = 0.0345$). These are the values at reference temperature (298 K) and assumed appropriate for the samples that spent several minutes at room temperature whenever they were sampled. The presence of bicarbonate ions is presumed to be negligible.

Measured, diluted and dissolved gas concentrations were multiplied with the appropriate volume (of water or headspace) to obtain absolute amounts in μg . The production rates were then calculated by dividing the change in carbon amount in headspace and water by the time since the last sample was taken, taking into account when a vial was flushed.

Missing data points were handled by removing them from the data set of concentrations, and calculating the production rates over the longer time span between the adjacent reliable measurements. Missing measurements from after the flushing of a vial were filled with the mean concentration of all post-flush measurements.

To correct for variabilities induced by the measurement, the production rates in the procedural blanks were subtracted from the production rates in the samples. This was only possible for CO_2 , as no measurable methane production occurred in the blanks.

Cumulative production and normalized rates

Finally, production amounts of single timesteps were added up to the cumulative production. Both cumulative production and production rates were normalized by dry weight [g] and organic carbon [g] (converted from %dw to g using the individual sample weight and water content per layer).

2.4.3 Derived metrics

The $\text{CO}_2:\text{CH}_4$ ratio was directly computed from the time series of cumulative production, normalized to g TOC.

To condense the total carbon loss into one number, the amounts of $\text{CH}_4\text{-C}$ and $\text{CO}_2\text{-C}$

were added up and normalized per g TOC.

To quantify the impact of incubation temperature in a simple form, the Q_{10} was computed as $Q_{10} = (R_2/R_1)^{10/(T_2-T_1)}$ from sample pairs which differed only in incubation temperature. This value describes the expected increase in respiration caused by a 10 K temperature increase (Hamdi et al., 2013). To cover the whole range of potential results, nine values per treatment group were calculated from all combinations of three plus three replicates.

To characterize the treatment effects on the time dimension, timing and magnitude of peak production rates were determined.

2.4.4 Fitting compartment models for decomposition

The organic origin of gaseous carbon observed in incubations can be conceptually divided into kinetic pools: a fast pool that dominates the initial carbon release, and a slow-cycling pool that becomes relevant once the labile carbon is depleted (Schädel et al., 2020). To estimate the fractionation into a labile and a stable fraction of carbon, a two-pool model with reciprocal exchange between the pools was fit for each treatment group. The model structure was constructed with the R package *SoilR* (Sierra et al., 2012) and fit to the observed carbon production using the Nelder-Mead optimization provided by *FME* (Soetaert and Petzoldt, 2010). The model represents decomposition abstractly as the exponential decay of two connected compartments, and contains no other process-based information.

A model consists of five parameters: the decomposition rates of the "fast" pool of labile carbon (pool 1) and the "slow" pool of recalcitrant carbon (pool 2), transfer coefficients between the two pools, and an initial fraction of carbon contained in the fast pool. The initial values are given in Table 2.4. The decomposition rates were estimated from average GHG-carbon flux rates in the first 60 days and the whole incubation time for pool 1 and 2, respectively. A small amount of 10% initial labile carbon and a very small exchange in both directions was assumed.

Separate models were fit to average cumulative carbon production per gram dry weight ($(\text{CO}_2\text{-C} + \text{CH}_4\text{-C}) \text{gdw}^{-1}$) of each treatment group. The resulting estimates of decomposition rates and transfer coefficients could then be analyzed for differences between treatment groups using Kruskal-Wallis tests.

parameter	meaning	initial value
k_1	decomposition rate of pool 1	0.01
k_2	decomposition rate of pool 2	0.005
α_{21}	transfer coefficient to pool 2 from pool 1	0.01
α_{12}	transfer coefficient to pool 1 from pool 2	0.01
γ_1	fraction of carbon contained in pool 1	0.1

Table 2.4: Parameters that are optimized in the two-pool decomposition model and their initial values.

2.5 Statistical analysis of treatment effects

Multiple linear models were built and compared with regard to how well they could explain normalized cumulative carbon production. The goal was to look for any statistical evidence whether:

- Nitrogen addition changes the amount of GHG production significantly,
- This trend is either negative or positive,
- the impacts of oxidized and reduced forms of N are not the same.

To investigate the effects of Nitrogen treatments and their form, either the total amount of $\text{NH}_4\text{-N} + \text{NO}_3\text{-N}$ was supplied as one explanatory variable (`total_N_ug`), or as two separate variables `NH4_N_amount` and `NO3_N_amount` (see Table 2.3) together with the incubation temperature `temp`. Additionally, similar models were built to quantify effects on sustained global warming potential and Q_{10} that included interaction terms. Diagnostic plots were employed to check for violations of the preconditions for linear regression. The response was log-transformed as that improved the normality of all models' residuals. Models were further assessed by explained variance (r^2) and compared by AIC. The coefficient estimate of each predictor was used to assess the effect size of each treatment and evaluate its statistical significance by the p-value.

Differences of model parameters between N treatment and temperature groups were tested with one-way Kruskal-Wallis tests.

3. Results

3.1 Sample properties

3.1.1 Chemical and physical properties of soil and pore water

The samples were oversaturated with water, as was evident during the preparation where pools of water formed at the bottom of their container. The carbon content was dominated by organic carbon, while the mineral fraction is negligible in comparison (Table 3.1). C:N decreases with depth, which is mainly due to a higher N content, as all other parameters differ only marginally. The BWT material was slightly denser and thus contained less water on a weight basis, despite its origin from below the water table.

	depth cm	%H ₂ O % ww	%TC %dw	%TOC %dw	%TIC %dw	%TN %dw	C:N	dry BD g/cm ³
AWT	0 - 3	97.3	42.0	41.9	0.125	0.628	70	0.0214
BWT	6 - 20	96.8	42.9	42.8	0.105	0.785	53.6	0.0339

Table 3.1: Peat properties: gravimetric water content, content of total carbon (TC), organic carbon (TOC) and inorganic carbon (TIC), total nitrogen (TN), carbon to nitrogen, and dry bulk density. C:N is calculated as total C divided by total N.

The pH of all water samples was acidic with a mean pH of 4.03 (Table 3.2), indicating that compounds are protonated in this environment. The presence of ions as indicated by electrical conductivity was low, decreasing with depth, and notably higher in the tap water that was used for creating treatment solutions. All of electrical conductivity, dissolved organic carbon and dissolved nitrogen showed a clear decreasing trend with depth/ decomposition stage.

	pH	EC $\mu\text{S}/\text{cm}$	DOC mg L^{-1}	TDN mg L^{-1}	C:N
AWT (0 - 3 cm)	4.02	347	1 130	23.8	47.5
_WT (3 - 6 cm)	4.04	119.1	457	5.72	79.9
BWT (6 - 20 cm)	4.03	64.6	186	3.28	56.7
tap water (stored)	7 to 8	554	NA	NA	NA
tap water (report)	7.7	550 - 800	1.7	NA	NA

Table 3.2: Water properties: pH, electric conductivity (EC), dissolved organic carbon (DOC), total dissolved nitrogen (TDN), and DOC:TDN.

3.1.2 Microbial community

Figure 3.1 shows the total number of *16s* copies, which indicate total microbial abundance, as well as gene copies indicative of methanogen and methanotroph presence (*mcrA* and *pmoA*, respectively) for each layer. Numbers are given as averages of replicates.

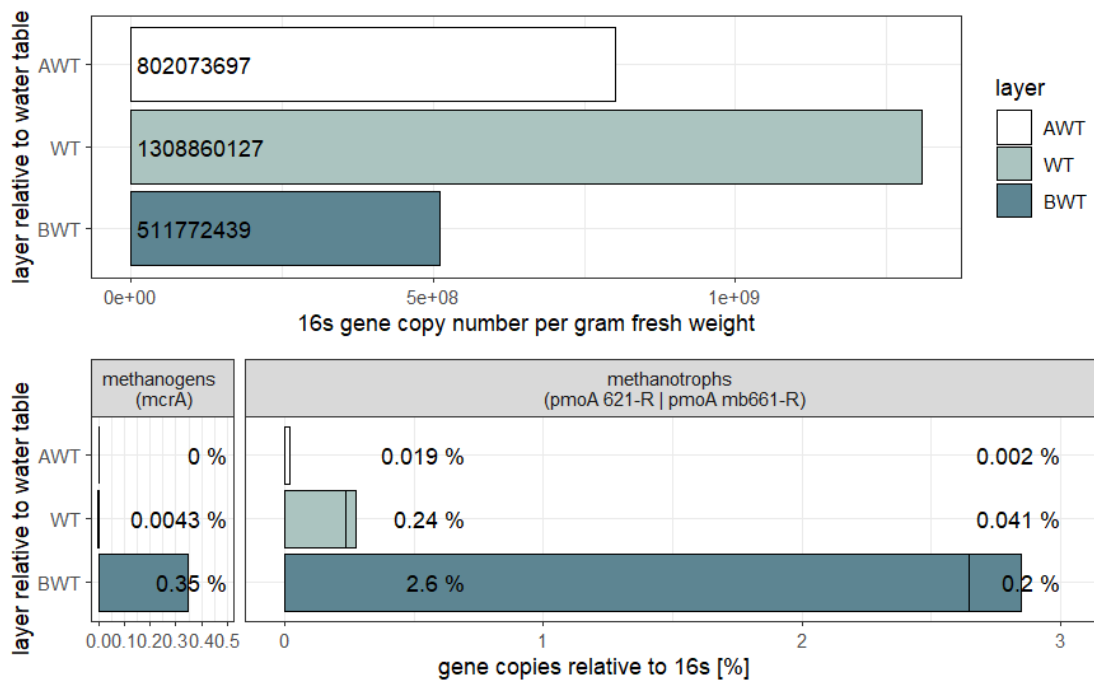


Figure 3.1: Gene copy numbers of *16s* g^{-1} fresh weight (upper panel) and of *mcrA* (bottom left) respectively *pmoA* (bottom right) relative to *16s*.

In general, microbial abundance peaks in the zone of fluctuating water table. Methane-related genes were more frequently expressed with depth (both on relative and absolute terms), and methanogens were completely absent in the top 3 cm. At every depth, methanotrophs were more numerous than methanogens.

3.2 Observed greenhouse gas fluxes

Blanks and measurement uncertainty

No trend was observed in the procedural blanks. Variations in blanks with and without N treatment solutions follow each other closely. This confirms that contamination with living organisms was avoided, and supports the assumption that blank data record methodical and measurement variations. On average, the concentrations varied by 140 ppm (one standard deviation of all measurements).

General observations

While CO₂ production set in immediately in the first week and then steadily decreased, methane production was observed only after several days, where it occurred at all: the surface samples exhibited no methane release until the end of this study.

A second productivity peak was observed in the AWT samples around day 60. The highest CO₂ production rate was 1271 μg CO₂-C gTOC⁻¹ d⁻¹ (532.3 μg CO₂-C gdw⁻¹ d⁻¹). Peak methane production amounted to 122.0 μg CH₄-C gTOC⁻¹ d⁻¹ (52.21 μg CH₄-C gdw⁻¹ d⁻¹). A high CH₄ production around day 10 to 60 is associated with a coincident or slightly preceding decrease in CO₂ concentrations.

Final carbon dioxide to methane production ratios ranged from 0.11 to 4.1 in the methane-producing samples. At its onset, of methane production is usually one or two orders of magnitude smaller than carbon dioxide production, but within the first two months, a much tighter ratio is approached that then remains mostly stable (see Figure 3.2).

In the subsequent text, cumulative productions are reported as means ± standard deviation unless indicated otherwise.

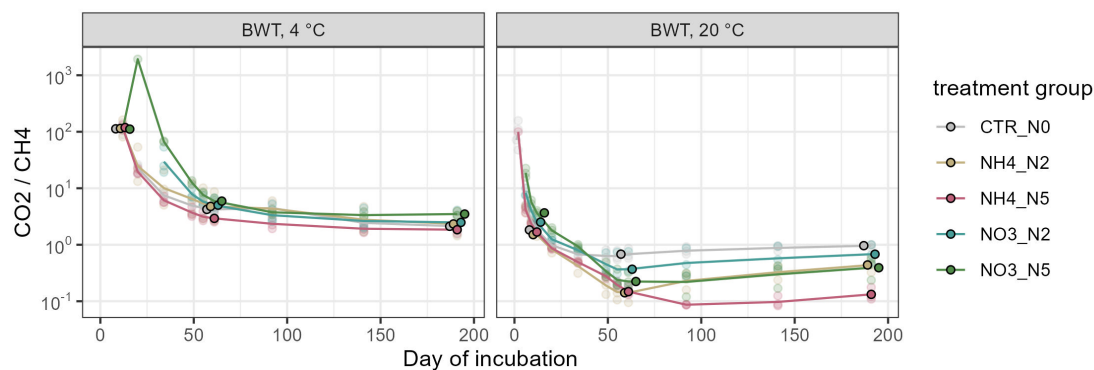


Figure 3.2: Time series of carbon dioxide to methane ratio in samples where methane was produced. Note that the vertical axis is logarithmic.

3.3 Effects of sampled layer

Potential GHG production in the 20 °C control group

The samples incubated at 20 °C under ambient nitrogen concentrations can provide an estimate of potential maximum GHG production of the Siikaneva bog material. After 190 days, a total of 14.6 ± 0.7 mg CO₂-C gTOC⁻¹ were produced in the surface layer samples, but no CH₄ production occurred at all. In the BWT samples, mean CO₂ production amounted to 6.7 ± 2.2 mg CO₂-C gTOC⁻¹, which was very similar to methane with 6.9 ± 1.9 mg CH₄-C gTOC⁻¹. This corresponds to approximately 1.5 % of TOC being released in the surface samples, and a very similar fraction of 1.4 % in the deeper layer, after 190 days under summer-like incubation temperature.

Timing and magnitude of peak carbon release rate

Peak CO₂ production was reached by day 7, on average; however, this differs between the subsurface samples, where the majority of samples start with peak production on day 1, and the surface samples, whose peak is slightly delayed to day 5 (median). After two weeks, surface samples had produced almost an order of magnitude more CO₂-C than subsurface samples in the same treatment group, a trend that continues through to two months and is only balanced out by strong BWT methane production. Peak methane production is reached after around 55 days (median, range of replicate means: 29 - 65 days).

As samples from the oxic surface layer and naturally waterlogged layer exhibited such different gas production behaviour, they were modelled separately in the subsequent

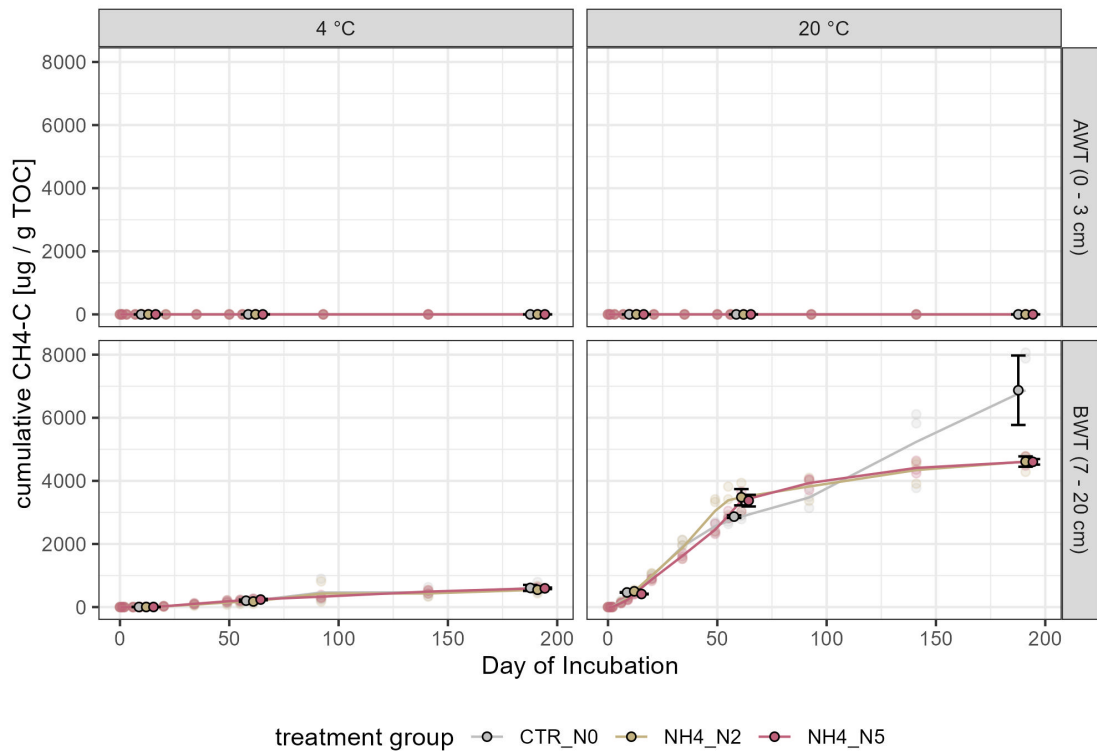
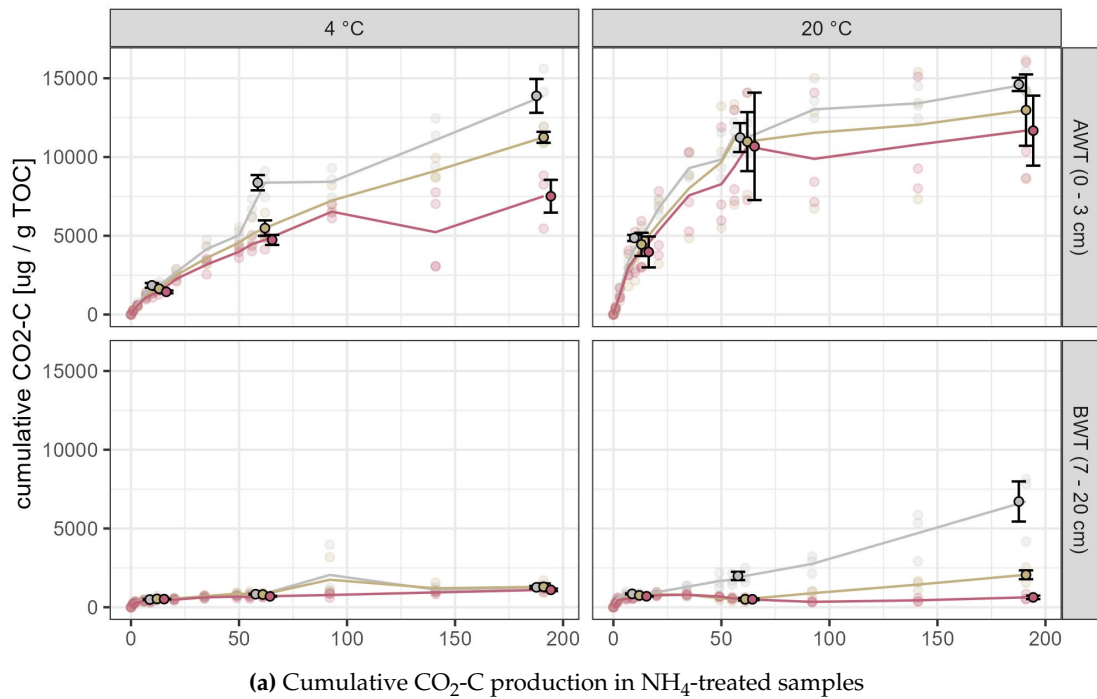
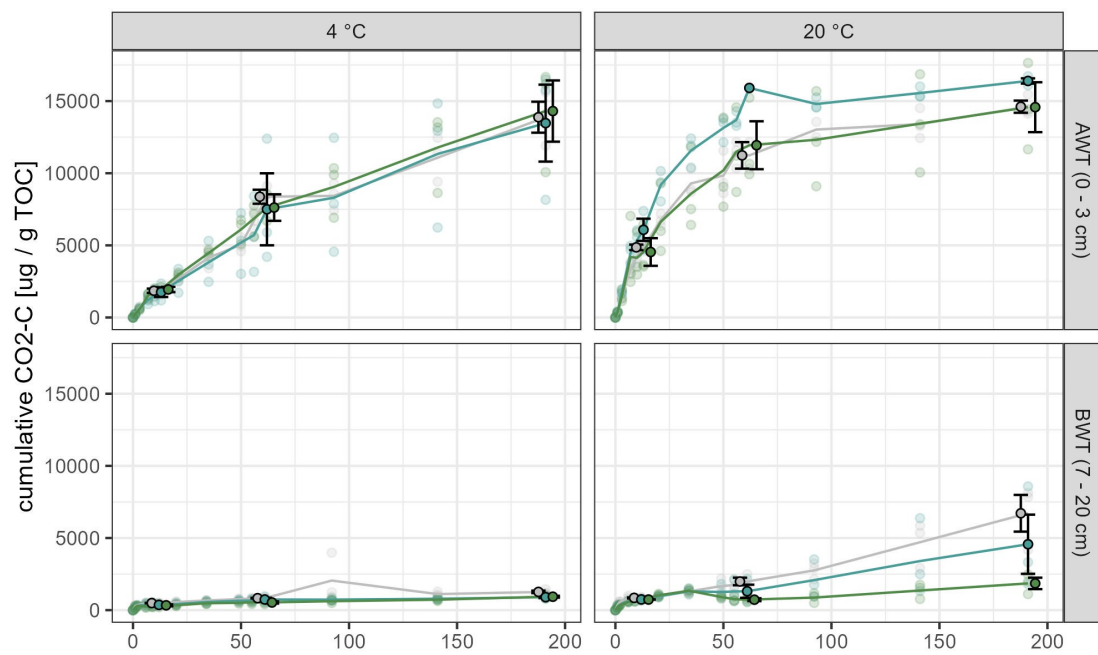
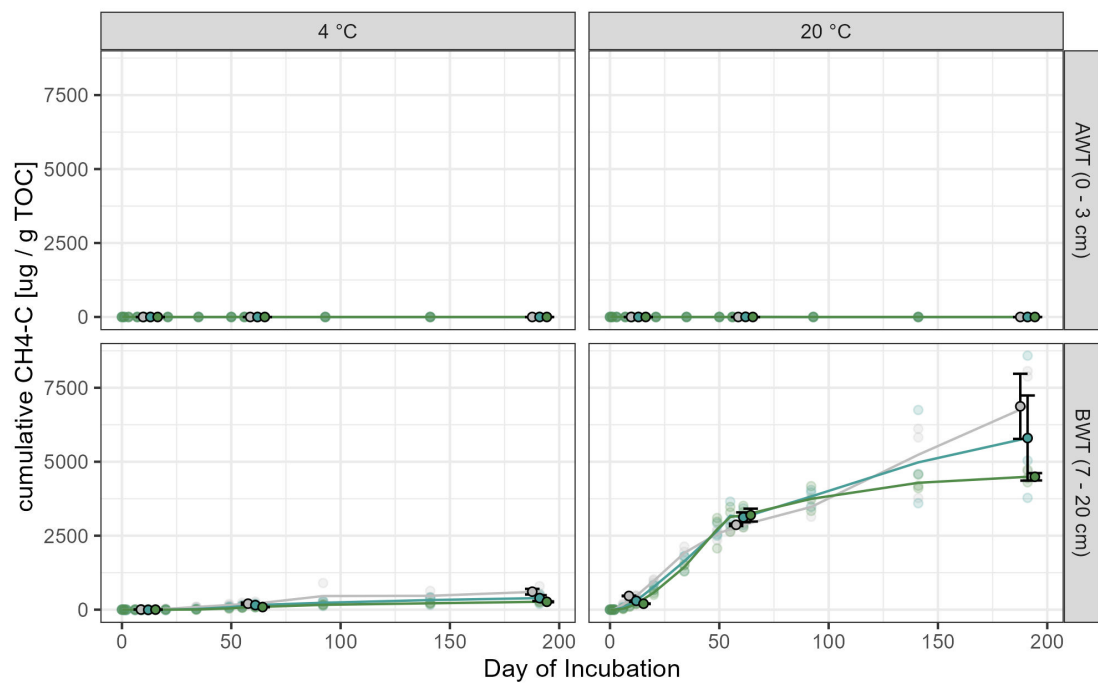


Figure 3.3: Development of cumulative carbon production over time in the samples treated with ammonium. Within each panel, colors compare N treatment level to the control. Individual samples' data are shown in transparent points and their means as lines. Solid points with errorbars show means \pm standard errors for each group at three time steps of interest. Points are shifted horizontally for better visualization.



(a) Cumulative CO₂-C production in NO₃-treated samples



(b) Cumulative CH₄-C production in NO₃-treated samples

Figure 3.4: Development of cumulative carbon production over time in the samples treated with nitrate. Within each panel, colors compare N treatment level to the control. Note that the control groups are shared between nitrate and ammonium treatments.

data analysis.

3.4 Effects of incubation temperature

Timing and magnitude of peak carbon production rate

In the second week of incubation (12 days), a clear temperature effect could be observed: carbon production in the 20°C vials consistently surpassed their 4°C equivalents. Methane production had started only in the 20°C incubation. However, CO₂ production was already quite active, leading to a high CO₂:CH₄ ratio. Consequently, peak carbon production rates of 20°C incubations were higher than of 4°C incubations. Over time, carbon dioxide release in the surface samples converged. Additionally, the temperature affected the trajectory of carbon production: at four degrees, it was more linear, while at 20 °C, it resembles a logarithmic curve. However, temperature had no significant effect on the day of peak carbon production.

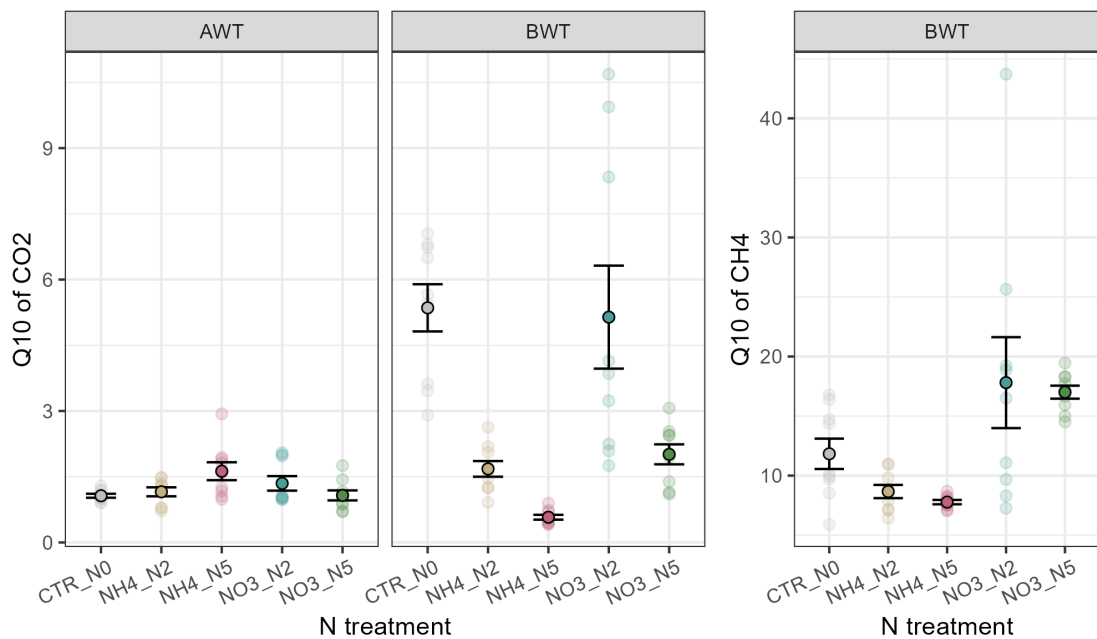


Figure 3.5: Q₁₀ of anaerobic carbon dioxide production (left) and methanogenesis (right) in the N treatment groups; mind the different scales of the vertical axis.

Cumulative carbon production Material from different positions relative to the water table showed very different responses to temperature. While the to-

tal C production in the AWT 4°C control group reached a comparable amount of $13.9 \pm 1.9 \text{ mg CO}_2\text{-C gTOC}^{-1}$ to its 20°C counterpart, production in the BWT group was reduced to $1.3 \pm 0.2 \text{ mg CO}_2\text{-C gTOC}^{-1}$ and, by an order of magnitude, $0.6 \pm 0.2 \text{ mg CH}_4\text{-C gTOC}^{-1}$ at 4 °C.

For anaerobic CO₂ production, the average Q₁₀ within the control group was 1.1 in surface-, and 5.4 in subsurface peat. The average over all samples was 2.1, with a range from 0.41 to 11 (Figure 3.5). In the linear models that accounted for N oxidation state, the effect of the warmer temperature treatment was a 19% productivity increase in the samples from above the water table. Samples from below the water table were more reactive to temperature: There, CO₂-C productivity exactly doubled from 4 to 20 °C.

Methanogenesis reacted more than twice as sensitively to temperature: the control group had a Q₁₀ of 12. Overall, values ranged from 5.9 to 44 with a mean of 13 Figure 3.5. Also, in the linear model, material incubated at 20 °C was estimated to produce 11 times more $\mu\text{g CH}_4\text{-C gTOC}^{-1}$ than at 4 °C. This estimate was stable across both total-N and N-species-specific models.

Total C loss Figure 3.6 shows the cumulative carbon production expressed as a percentage of initial TOC. While most treatment groups range within a similar magnitude, the material from below the water table that was incubated at 4 °C stands out with values that are 5 to 10 times lower.

Because of the behaviour of the 4°C BWT group as seen in Figure 3.6, it seemed appropriate to include an interaction term between layer and temperature in the linear model. This interaction was highly significant, and implied that temperature was 4.2 times more influential in the BWT samples. The temperature term itself was not significant, but the layer term indicates that peat from the anoxic zone released only a tenth of the carbon originating from the surface.

CO₂:CH₄ The ratio between the two greenhouse gases approaches a stable value in the second half of the experiment that differs significantly between incubation temperatures: At 4°C, the average CO₂:CH₄ ratio is 2.55, while at 20°C, it is 0.54.

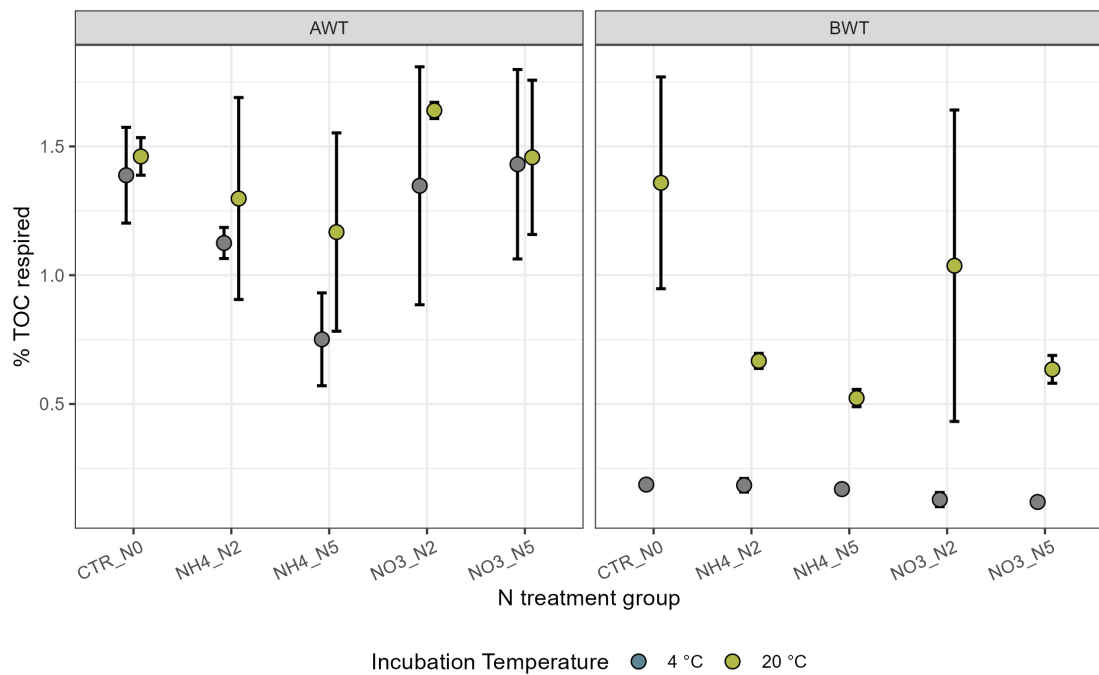


Figure 3.6: Comparing final proportions of TOC respired between treatment groups. Points with errorbars indicate means with standard deviations. Colors differentiate incubation temperature, the panels between peat depths.

3.5 Effects of nitrogen treatments

3.5.1 Total amount of N added

Cumulative carbon production

In exploratory plots, no clear relationship of carbon mineralization with total N application appeared. Linear models of carbon dioxide production were either insignificant as a whole (CO₂-C, AWT) or left residual patterns that point to unexplained additional factors. This indicates that either, N addenda had no effect at all, or that the form (oxidized/ reduced) of N determines its influence.

However, log-transformed CH₄-C production is well represented ($R^2 = 0.95$) by temperature and total N addition. According to this model, adding one μg of N in any form results in a significant 2% reduction of methane release. It must be noted that the good model fit is probably caused by the strong temperature effect that dominates the variance in this model.

Other parameters

In general, total N load appeared to be a suboptimal linear predictor of most quantities of interest: It had no significant effect on the timing and magnitude of peak carbon production rate. In the model of total C loss, the nitrogen term was not significant. Additionally, the model where N treatments were supplied as two different variables performed slightly better in terms of R^2_{adj} and AIC.

Figure 3.2, where nitrogen treatments are ordered by the total amount of N from left to right, does not indicate that Q10 would be modelled well by a linear regression of the total nitrogen amount.

3.5.2 Oxidation state

In general, comparing treatment sets within each N form, temperature and soil layer shows that higher treatment amounts either resulted in decreased C mineralization, or no conclusive trend at all.

In the following, results from modelling carbon release and derived quantities based on the predictors amount of $\text{NH}_4\text{-N}$, amount of $\text{NO}_3\text{-N}$ and temperature are reported. In all models, the diagnostics were improved by log-transforming the response (greenhouse gas production in $\mu\text{g C per g TOC}$).

Cumulative carbon production

$\text{CO}_2\text{-C}$ release in the AWT samples was predicted moderately well by its model ($R^2 = 0.46$). Ammonium addition and temperature were significant linear predictors at the 5% confidence level, but nitrate-N was not. For every additional μg of ammonium-N, a 5% reduction in carbon dioxide production was estimated. For the peat from below the water table, all three predictors were significant, and 56% of total variance could be explained by the model. Both forms of N reduced CO_2 production, namely by 13 % per μg ammonium-N and 3% per μg nitrate-N.

Methane production was very well explained by the model ($R^2 = 0.95$), but again, this result is dominated by a very high temperature effect. In this case, only nitrate resulted in a significant productivity decrease, which was estimated to 2 % per μg $\text{NO}_3\text{-N}$. (The factor for ammonium-N was almost identical but not significant.) This difference appears after day 60 when higher NO_3 addenda reduce the production rate compared to the control.

Proportion of C respired

The model which included N addenda as two numerical variables $\text{NO}_3\text{-N_amount}$ and $\text{NH}_4\text{-N_amount}$ explained 92% of the total variance of carbon mineralization. Both N addenda had a statistically significant impact: Adding ammonium decreased C release by 5% and nitrate by 1% per $\mu\text{g N}$.

Timing and magnitude of peak carbon production rate The CO_2 peak production was significantly sped up in the surface samples by both ammonium (3 days per μg) and nitrate (0.9 days per μg). The treatments primarily affected the magnitude of the second productivity peak. Contrastingly, there was no effect of the addenda on the $\text{CO}_2\text{-C}$ peak timing in the BWT samples. After two months, the NH_4 addenda strongly reduced $\text{CO}_2\text{-C}$ and simultaneously increased $\text{CH}_4\text{-C}$ production in the samples from the waterlogged layer. This effect was large enough that 20°C incubated samples that were treated with ammonium then fell behind 4°C samples in terms of carbon dioxide production. For surface peat, a moderate increase of nitrate seemed to stimulate the release of carbon dioxide, although this effect was not reproduced under colder temperatures. There, ammonium addenda resulted in less carbon dioxide.

For methane, coefficients of all N treatments on the day of peak production were positive but insignificant. There appeared a positive linear relationship between peak timing and magnitude. On the short term, elevated NO_3 clearly reduces methanogenesis - the N5 treatment emitted less than half as much C as the control group (at 20°C , CTR $463.8 \pm 17.6 \mu\text{g CH}_4\text{-C gTOC}^{-1}$ vs. N5 $200.4 \pm 16.6 \mu\text{g CH}_4\text{-C gTOC}^{-1}$.) - but only for a few weeks.

$\text{CO}_2\text{:CH}_4$ ratio The availability of nitrate initially increases the ratio. In the 20°C incubation however, it falls below the control treatment after around 40 days.

Additionally, a pronounced decrease in the 20°C ammonium treatment group appears (Figure 3.2). NH_4 (and in less clear form, NO_3) changes the shape of the $\text{CO}_2\text{:CH}_4$ time series curve, adding in a second drop around day 40 (20°C only), whereas the control treatment follows a nearly perfect negative exponential in logarithmic space. This leads to a significant effect of the N treatment on the final ratio in the 20°C incubation (Kruskal-Wallis test). Again, this emphasizes an intermediate period where CO_2 declines while $\text{CH}_4\text{-C}$ production accelerates.

3.5.3 Impact of N treatment on temperature sensitivity

The temperature sensitivity of carbon dioxide production was also impacted by the Nitrogen addenda. As Figure 3.5 already indicates, the direction and magnitude of this impact diverges according to position relative to the water table. A linear model that included an interaction term of ammonium- and nitrate-N-additions with the layer achieved an R^2 of 0.75 and was much more informative than one without (AIC: 164 vs. 86.1). The interaction of layer and ammonium resulted in a shift of direction: while in the surface samples, $\text{NH}_4\text{-N}$ was estimated to increase temperature sensitivity by 3.3%, the resulting effect in the subsurface samples was a 22% decrease in sensitivity. Nitrate attenuates Q_{10} significantly in the subsurface samples only (factor 0.968).

For methane, no such interaction was calculated but the fundamental difference between the layers is clear from the lack of methanogenesis there. Both N treatments were significant, but in different directions. NO_3 boosted the temperature response by 1.5 % per $\mu\text{g N}$, while $\text{NH}_4\text{-N}$ dampened it by 4.4%.

3.6 Results of fitting decomposition models

The model fitting process resulted in twenty different outputs (Figure 3.7). Two models didn't converge (AWT 20°C $\text{NH}_4\text{ N2}$, BWT 4°C control), and two had parameter estimates that departed unrealistically much from the bulk of all models (AWT 4°C $\text{NH}_4\text{ N2}$ and BWT 20°C $\text{NO}_3\text{ N5}$, marked red in Figure 3.7). All other models estimated a mean release rate of 0.66 d^{-1} from the fast and 0.016 d^{-1} from the slow pool.

In most models, the cumulative release from the fast pool plateaus after less than a week, and the overall release was dominated by the slow pool. (For a visualization of the individual model outputs, see appendix A.4).

In both layers, the slow pool in the 20 °C incubations was more active than at 4 °C ($p=0.09$). In the surface samples however, the fast pool was slower and the initial fraction of fast material was also considerably larger.

A consistent acceleration of the decomposition rate of the fast pool with increasing N addenda can be observed in the 20°C AWT ammonium treatment and the 4°C BWT nitrate treatment. In a Kruskal-Wallis test, no differences of any of the five fitted parameters between N treatments were found to be significant. However, statistical tests were impaired by the fact that results from some treatment groups could not be considered, especially the BWT 4°C control group. Furthermore, the residuals are quite large, indicative of a poor fit. In some cases, root mean square residuals approach

treatment group	k_1	k_2	α_{21}	α_{12}	γ	R.M.S.R.	cum. C	SE
AWT_04_CTR_N0	0.387	0.016	1.6%	1.4%	2.5%	2.20	5.81	0.45
AWT_04_NH4_N2	98.982	0.014	97.1%	0.6%	1.3%	1.73	4.71	0.15
AWT_04_NH4_N5	0.498	0.010	0.9%	1.5%	3.9%	0.84	3.15	0.44
AWT_04_NO3_N2	0.364	0.014	2.2%	0.8%	3.2%	0.62	5.64	1.12
AWT_04_NO3_N5	0.345	0.017	26.2%	0.6%	2.9%	1.30	5.99	0.89
AWT_20_CTR_N0	0.040	0.039	1.0%	1.0%	12.1%	5.57	6.12	0.18
AWT_20_NH4_N2	0.044	0.043	1.0%	1.0%	12.1%	0.68	5.44	0.95
AWT_20_NH4_N5	0.113	0.039	1.0%	1.0%	9.5%	0.38	4.89	0.93
AWT_20_NO3_N2	NA	NA	NA	NA	NA	-	6.87	0.08
AWT_20_NO3_N5	0.039	0.038	1.0%	0.9%	14.6%	1.43	6.11	0.72
BWT_04_CTR_N0	NA	NA	NA	NA	NA	-	0.80	0.04
BWT_04_NH4_N2	1.060	0.001	0.7%	1.9%	3.2%	2.07	0.79	0.07
BWT_04_NH4_N5	0.787	0.001	1.1%	1.1%	3.8%	1.64	0.73	0.03
BWT_04_NO3_N2	0.892	0.001	1.1%	1.2%	3.2%	1.25	0.55	0.07
BWT_04_NO3_N5	1.665	0.001	1.1%	1.5%	2.7%	0.75	0.51	0.03
BWT_20_CTR_N0	1.212	0.009	1.4%	0.9%	4.0%	1.44	5.82	1.02
BWT_20_NH4_N2	0.299	0.006	1.1%	1.0%	6.5%	1.47	2.86	0.07
BWT_20_NH4_N5	0.678	0.006	1.3%	1.3%	3.8%	4.04	2.24	0.08
BWT_20_NO3_N2	2.058	0.009	0.9%	4.5%	1.8%	0.81	4.44	1.49
BWT_20_NO3_N5	0.012	0.000	0.4%	0.3%	71.6%	4.05	2.72	0.13
mean (valid models)	0.655	0.016	2.7%	1.3%	5.6%	1.66	3.82	0.53

Figure 3.7: Modelled decomposition rates [d^{-1}], exchange ratios and labile fraction for all treatment groups, as well as the square root of mean square residuals ($mg\ C\ gdw^{-1}$). Mean and standard error of cumulative C release on the last day are also provided as a reference. Models that did not converge or were considered unreliable are marked in red. Grey bars give an indication of a cell's value relative to the other values in the same column.

(AWT_20_CTR_N0) or even surpass (BWT_20_NH4_N5) the mean cumulative C release of the treatment group. Many models underestimate production, particularly towards the end of the incubation.

4. Discussion

4.1 Position relative to the water table and microbial community

Like Currey et al. (2009), this study found stronger effects of depth (i.e., position relative to the water table and decomposition state) compared to N load or form.

The hypotheses (section 1.2) predicted a longer time lag until the onset of methane production for the samples from above the water table, where the decomposer community would be less adjusted to the anoxic conditions in the incubation vial. In practice, methane was not produced by the surface samples until the end of the experiment, while the sub-surface peat exhibited instant and productive methanogenesis. The complete lack of detectable methanogens in the surface peat explains why no methane was produced there (Figure 3.1). Therefore, two fundamentally different metabolic systems define these layers, which is not surprising given that they were chosen to represent two naturally different environments.

Although periodically limited oxygen supply at the surface is part of the seasonal cycle in Siikaneva, when the bog is covered in snow in winter and subsequently flooded by meltwater, methanogenic microbes were not established there. The microbial community was not at a steady state under anaerobic conditions (Nilsson and Öquist, 2009, p. 136), had to adapt more than the community from below the water table (as indicated by longer lag times), and results might deviate further from real-world conditions. Even below the water table, methanotrophs were more abundant than methanogens. Thus the sampled depth of 7-20 cm probably did not reach completely anoxic conditions.

A substantial delay of the methane peak was also observed in other studies (Knoblauch et al., 2013). As methane production did set in after a few days only, the presence of more favourable electron acceptors suggests itself as the most likely explanation for the delay, as sufficiently reducing conditions had to be reached first.

Samples from above the water table had more favourable stoichiometry in the water, but less so in the bulk C:N. This divergence is interesting, because it indicates that the release of cell material by frost damage was not ample enough to align the liquid C:N to the same as in the solid material. Even though two samples provide insufficient support to draw conclusions on the substrate effects on production, it may explain why there was no notable difference between the layers in the final proportion of TOC that was released: While the BWT microbial community faced familiar conditions, decomposers above the water table had superior substrate (assuming that dissolved C and N are more available to microbes, compare L. Chen et al. (2018)). These geochemical results were not represented in a larger fast pool of the surface samples in the decomposition models. This may be a misrepresentation or reinforce the aforementioned point that the surface microbial community was not equipped to access the full carbon reservoir. In fact, production rates levelled off substantially in the AWT samples after just a few months, while the control of BWT was still active.

Wilmoth et al. (2021) stress that fluctuating oxygen supply greatly (2000 times!) enhances methane production during anoxic conditions, due to functional shifts between different microbial communities. The microbial assay also detected the highest amount of (unspecified) bacteria in the WT layer, which wasn't incubated. Because its boundaries were hard to delineate in the field, the material which was clearly in a fresh or decomposed state, respectively, was prioritized.

4.2 Temperature reactivity

As hypothesized, higher temperatures resulted in higher production rates for both observed greenhouse gases. The reaction was more extreme for methanogenesis and drives a pronounced difference in total carbon release between the two peat depths that were sampled: production in peat from below the water table is much more sensitive to temperature.

Mean Q_{10} for CO_2 was within the typical range for peat samples (Hamdi et al., 2013; Treat et al., 2015). However, this average interpolates between a rather low reactivity in the above water table, where cumulative carbon production hardly differed between the cool and warm incubation, and a rather high value of 5.4 below the water table. Another study of Siikaneva peat found a much lower $Q_{10}(\text{CO}_2)$ of 0.6 - 0.8 (Baysinger et al., 2024), and their deep peat (30-50 cm) was even less sensitive. This agrees with the surface samples here, but contrasts the highly temperature-driven below water table emissions in this study.

For methanogenesis, a higher Q_{10} was expected (Nilsson and Öquist, 2009), but the results exceeded those of Treat et al. (2015) multiple times (median: 1.16, range 0.96 - 3.10, here: control group average of 12). A possible explanation could be that they summarized studies of permafrost soils with a markedly lower organic fraction, i.e. less substrate to support a large reactive decomposer community. Moreover, the values presented here may be somewhat inflated as they were derived from individual measurements rather than averages, but the control group values are not highly skewed.

As expected, higher temperatures shifted the ratio of $\text{CO}_2 : \text{CH}_4$ towards CH_4 . Its final value drops below 1 only at 20°C, which would have been the expectation for ideal methanogenic conditions (Nilsson and Öquist, 2009, p. 135).

That temperature also modifies the shape of the time series (most evident in 3.4a) reflects the fact that higher temperatures result in a faster depletion of available substrate. The decomposition models partly attribute this to an accelerated turnover of the slow pool. While initial rates in the warmer temperature groups are much higher, final carbon release is equally around 1.5% in the AWT samples. This may represent the size of a limited accessible carbon pool that all samples have in common (Figure 3.6). Samples inhibited by Nitrogen addenda or lower temperatures (BWT) did not achieve their full potential to mineralize this pool. The decomposition models' mean estimate of 5.6% labile carbon is somewhat higher but also unstable, as it varies between 1.8% and 14.6%. Interestingly, a larger carbon fraction was assigned to the labile pool under warmer temperatures, where more "difficult" substrate may become accessible. Note also that the slow pool in these models does contribute to carbon release and does not represent an inert carbon stock.

4.3 Nitrogen addenda

N additions were hypothesized to lead to higher respiration. However, the opposite effect was observed in the experiment: The only statistically significant effect of N load was an inhibition of methane production. This contrasts the initial hypothesis that lifting a proposed N limitation of decomposers in Siikaneva bog would allow them to mineralize higher amounts of carbon, but other studies have also found similar results: For example, N additions impaired basal respiration in the denitrification study of Francez et al. (2011) (methane production was unaffected). Breeuwer et al. (2008) also found no effect of N deposition levels on sphagnum mass loss in litter bags, and not of temperature, either. In an anaerobic setting, Kim et al. (2015) connected an observed inhibition of methane release by N and P supply to competition with denitrification.

Furthermore, N addenda may have nonlinear effects: Contrary to all other treatments, low N deposition - doubling ambient atmospheric input - in Currey et al. (2009) did not stimulate carbon turnover. Transferred to this study, the treatments may have been too conservative. But they oriented their treatments on atmospheric deposition and applied them in a natural ecosystem, whereas this study uses the much larger natural N stock and traps the N in the incubation vial, so the N₂ treatment here should surpass the "low" range in Currey et al., 2009.

These results suggest that viewing decomposition through the lens of nitrogen limitation is not ideal for advancing the understanding of peatland greenhouse gas emissions. A second important finding was that the oxidation state of N addenda shapes the reaction of carbon release. Contrary to the initial assumption, nitrate did not affect decomposition more than ammonium, but rather, production in ammonium-treated samples was more strongly reduced than in those with nitrate treatment. This confirms the findings of Currey et al. (2009), who found significant results only for ammonium.

The fact that total N load was not a good linear predictor, even though both forms of addenda had inhibiting properties, could mathematically be explained by the fact that the N effects have different slopes, that were observed at different points (i.e. nitrate effects are less drastic, but higher amounts of N were added as nitrate).

The following paragraphs will explore several processes that potentially contributed to the results.

4.3.1 NO₃ as competing terminal e⁻-acceptor

Nitrate mainly impacted methanogenesis - an expected result, as alternative electron acceptors like nitrate "competitively inhibit methanogenesis and support anaerobic methane oxidation" (AMAP, 2015, p. 16). Nitrate as the most energy-efficient oxidant after molecular oxygen is depleted first, followed by manganese, iron and sulfate, via pathways that release carbon as CO₂, before methanogenic conditions are reached. This lag phase shortens with higher temperatures that speed up decomposition (Reddy et al., 2023, p. 184). Indeed, a lag of several days before the onset of methane production was observed in this incubation that also differed between temperatures (section 3.3). Nitrate addenda did have a significant diminishing effect on carbon production in the samples from below the water table that develops around day 50 (Figure 3.4a, 3.4b). However, a temporarily limited competition of other electron acceptors with methanogenesis should result in cumulative respiration curves that diverge between treatments, but then continue in parallel once the alternative acceptors are depleted, and this is not the case. Why nitrate did not significantly affect carbon dioxide production in the

samples from above the water table is not clear, as carbon dioxide-producing electron pathways are also less favourable than nitrate. The large within-treatment variation definitely impacted the associated statistics, but the high cumulative production of the 20°C N₂ treatment could point to a nonlinear response that would not have been accurately represented by linear models. In general, NaNO₃ impacts were potentially buffered by the pH increase that they cause by replacing H⁺ with Na⁺ ions (Currey et al., 2009).

Therefore the presence of alternative electron acceptors can't fully explain the observed trends. However, looking at the data from this angle might provide some further insights into the actual processes that shaped them.

Firstly, other alternative terminal electron acceptors were likely present. For example, sulfate-reducing microbes transform sulfate to hydrogen sulfide (H₂S). This gas was not measured in the headspace samples, but a smell was perceptible whenever the incubation vials were flushed fits the description of the foul odor of hydrogen sulfide. Around 10.95 µg g⁻¹ SO₄²⁻ can be expected in bog water, which is an order of magnitude more than the nitrate found in the same study (H. Zhang et al., 2021) and considerable amounts were added with the tap water. Therefore sulfate reduction probably took place in the incubation as well and competed with methanogenesis. Furthermore, as it facilitates anaerobic methane oxidation (Raghoebarsing et al., 2005), some methane may have been consumed as well.

Secondly, CO₂ and methane that are produced in acetotrophic methanogenesis (produces CO₂) should be impaired by nitrate additions similarly. But if nitrate metabolism outcompetes hydrogenotrophic methanogenesis (which consumes CO₂), it should be expressed by higher CO₂ and lower CH₄. The CO₂ and CH₄ release rates were generally correlated. However, between day 20 and 50 the onset of methanogenesis was preceded by a decline in CO₂ concentrations. This points to a methanogenic pathway that uses CO₂ as substrate (hydrogenotrophic methanogenesis), unlike in the permafrost incubation of Knoblauch et al., 2013 where they increased together. In Figure 3.2, the nitrogen-treated samples exhibit a bulge and subsequent drop of CO₂:CH₄ that would indicate an initial stimulation and subsequent inhibition of hydrogenotrophic methanogenesis, or alternatively, a shift of the methanogenic pathway. Another hint on the tight connection of carbon release pathways are given by N effects on Q₁₀ (section 3.4) that were more consistent between the greenhouse gases within one layer, than for CO₂ across the two layers.

The nitrate treatments were probably lost quickly to denitrification and DNRA. For example, Francez et al. (2011) observed that denitrification was stimulated by nitrate

treatments, and depleted their nitrate addenda within less than 10 days. In this study, NO_3 treatments ceased dampening methanogenesis around day 40. Therefore, competing metabolic pathways can explain initial effects of nitrate until its depletion, but another process has to underlie the subsequent second decrease.

4.3.2 Toxicity of addenda or intermediate products

Toxicity of ammonium for methanogens is a known issue from biogas production (Y. Chen et al., 2008). Concentrations that are discussed in that context surpass those of bog samples by several orders of magnitude: 200 mg L^{-1} are regarded as beneficial for methanogenesis, and toxicity research operates at scales of g L^{-1} and higher. However, communities adapted to nutrient-scarce bogs might still be impacted by much lower levels, and this could explain that ammonium inhibited GHG production in this experiment. An argument in favour of this theory would be that ammonium severely dampened the temperature response of samples from below the water table, where initial concentrations were probably already higher.

For nitrate, the toxic intermediate products of denitrification - dinitrogen oxide, nitrous oxide and nitrite - could have impacted the methanogen community (Bodelier and Steenbergh, 2014). It seems reasonable that larger quantities of those would be produced from higher loads of $\text{NO}_3\text{-N}$, resulting in the observed effect. Additionally, it is transformed to ammonium under reducing conditions.

Instantaneous toxicity should result in lower production rates in general but secondary products could build up over time, as incubation vials encapsulate a closed system where any metabolites accumulate (e.g. also H_2S). This matches the ongoing effect of the treatments as represented in diverging cumulative C production curves. Potential other influences could be by Sodium and Chloride in the treatments or the accumulation of excess H^+ over time.

4.3.3 Carbon use efficiency improved by nitrogen

Schimel and Weintraub (2003) argued on the basis of a microbe-focused decomposition model that alleviating N limitation would result in reduced respiration, as microbes would direct more carbon towards biomass growth when their N demand was fulfilled, and less would be respired through "overflow metabolism". They argue that a decrease in respiration after a pulse addition of N is no proof that microbes were not N-limited. Concurring empirical evidence has been found in thawing permafrost (L. Chen et al., 2018). If this was the driving mechanism in this experiment, N-amended incubation

vials should contain higher microbial biomass and a tighter C:N ratio. However, this could not be tested within the scope of this thesis, as the incubation was still ongoing. Furthermore, this theory can not explain differences between ammonium and nitrate treatments.

4.3.4 Colimitation

While N is a key nutrient, other limitations may also restrict microbial decomposition that have not been explicitly addressed in this experiment (Bobbink et al., 2022). In general, K and P are known to mitigate the N impact on *Sphagnum* (Carfrae et al., 2007). Nitrogen additions only boost methane release if combined with P and K supplementation (Juutinen et al., 2018). Enhanced decomposition induced in a whole-ecosystem warming experiment caused N and P availability to increase simultaneously (Iversen et al., 2023).

In the presented experiment, the N:P ratio was somewhat unnaturally widened in stronger treatments, as P was added at uniform levels with the tap water while N was varied. With % P = 0.017 (Korrensalo et al., 2018, 0 - 20 cm of *sphagnum* lawn) the background N:P would be between 37 and 46.

To conclude, co-limitation would be a potential explanation for missing effects of N addenda, but not inhibiting effects. These could be the combined outcome if microbes experience concurrent impacts of ongoing nutrient limitation and competition or exposure to toxic environmental conditions.

4.3.5 Diverging effects of N on the slow and fast C pool

Some studies suggest that N addenda have contrasting effects on organic matter in different stages of decomposition or of different degrees of recalcitrance: N addenda stimulated labile carbon decomposition, but reduced processes related to the decomposition of more complex carbon compounds. Their line of reasoning is that N supply makes respiration more productive, but relieves microbes of the need to decompose complex molecules to access the nitrogen therein. Measures of enzyme activity partly support this theory (Currey et al., 2009; Lavoie et al., 2011). Alternatively, N availability could stimulate complex organic matter decomposition by improving decomposer nutrient status.

In this study, any initially available labile carbon had several months to be depleted while the samples were stored at 4°C. Therefore, the carbon mineralized during the incubation may be sourced mainly from a slow pool, with some additional labile in-

puts that were introduced with the water treatment or released by disturbance when the experiment was launched. Following the aforementioned reasoning, N-amended samples should have a higher turnover rate in a small fast pool, but a lower rate in the slow pool. The two-pool decomposition models (subsection 2.4.4) were an attempt to explore this but did not yield any significant differences between treatment groups. Furthermore there were several indicators that the models were not reliable enough to confirm or deny hypotheses: the volatile estimate of labile pool size, large residuals, underestimation of production rates, and a high sensitivity to initial parameters during the fitting process (not shown).

4.4 Interactions

Multiple interactions were observed between the drivers of decomposition in this study and others before (Lavoie et al., 2011). For one, ammonium affected CO_2 -C release from below the water table more strongly than that from above, and nitrate effects were only significant there. Interestingly, nutrient release during experimental warming has also been observed to increase with depth (Iversen et al., 2023, depths of 30, 60 and 90 cm). Moreover, subsection 3.5.3 showed that N addenda affected the temperature sensitivity of anaerobic decomposition. NO_3 boosted the temperature response of CH_4 production, which agrees with what H. Zhang et al. (2021) found for the combined availability of several nutrients. A simple explanation for this could be a higher abundance of methanogens under improved nutrient supply (Martí et al., 2019). However, NH_4 had the opposite effect in this study.

The observed temperature response of methanogenesis might also just represent that of nitrate cycling: higher NO_3 levels support a metabolism that competes with methanogenesis (reduction to gaseous N or ammonia), which in turn occurs faster under higher temperatures, leading to a quicker loss of nitrate and stronger onset of methanogenic conditions.

4.5 Realism and representativeness

4.5.1 Sample properties

The sample properties described in section 3.1 largely agreed with other studies done in Siikaneva (Mathijssen et al., 2016; Korrensalo et al., 2018). We can therefore rely on these results to be typical for this material. One notable difference lies in the wider C:N ratio of the surface layer samples (70), which are from fresh sphagnum and not

comparable to peat in further stages of decomposition (typical range: 40 -60, Amelung et al. (2018)).

Siikanevas microbial community appears to be exceptionally rich in methanogens and poor in methanotrophs compared to other Finnish bogs (H. Zhang et al., 2021). This study can not confirm this proportion, as it counted more methanotroph than methanogen genes (subsection 3.1.2). In a more detailed microbial assay of Siikaneva peat, a substantial amount of methanogenic archaea within the top 30 cm was identified as the group *Rice Cluster II*. In general, the microbial community was distinct from adjacent forest and intermediate ecosystems and included *Acidobacteriota*, *Syntrophobacteraceae* (*Desulfobacterota*), and several phyla of *Proteobacteria* (*Isosphaeraceae*, *Pirellulaceae*, *Acetobacteraceae* and *Beijerinckiaceae*). Methanotrophs decreased substantially in abundance below 30cm, but so did methanogens (Baysinger et al., 2024, *in review*).

4.5.2 Carbon fluxes

Material from Siikaneva bog has previously been incubated by Baysinger et al. (2024, *in review*). After 140 days, cumulative production amounted to $3\,150\ \mu\text{g CO}_2\text{-C gTOC}^{-1}$ in the 4°C incubation of material from 0-30cm depth. This amount of $\text{CO}_2\text{-C}$ clearly surpasses the production of BWT at 4°C in this study ($468 \pm 147\ \mu\text{g CO}_2\text{-C gTOC}^{-1}$), is comparable to 20°C BWT production ($5\,236 \pm 1\,274\ \mu\text{g CO}_2\text{-C gTOC}^{-1}$), but below the 4°C AWT results ($11\,077 \pm 1\,544\ \mu\text{g CO}_2\text{-C gTOC}^{-1}$) (mean cumulative production after 141 or 142 days in the control group). Methanogens were not reliably established in that experiment. The 30-50 cm peat samples were "unresponsive" to temperature treatments and produced significantly less $\text{CO}_2\text{-C}$.

Concerning methane, samples in this thesis experiment were at least three times more productive than northern bog samples in H. Zhang et al. (2021). Within 9 days, BWT samples in the control group released $79\ \mu\text{g CH}_4\text{-C gdw}^{-1}$ on average, which equals $8.8\ \mu\text{g CH}_4\text{-C gdw}^{-1}\ \text{d}^{-1}$ compared to $< 1.8\ \mu\text{g CH}_4\text{-C gdw}^{-1}$. Mean methane oxidation rates under aerobic conditions in the same study were at $12.6\ \mu\text{g CH}_4\text{-C gdw}^{-1}\ \text{d}^{-1}$. While these numbers can not be used to calculate a methane balance as they originate from different incubation conditions, this still highlights a substantial potential for methane uptake of this peat.

Total carbon release also remarkably surpassed that of a long-term incubation of permafrost samples (Knoblauch et al., 2013), where 0.27–1.16% (average 0.55 +- 0.23%) were mineralized as CO_2 under anaerobic conditions within a much longer period of 1200 days. The amount of methane released from those samples with active methanogenesis accounted for 0.005–0.83% (average 0.28 +- 0.23%) of initial carbon. This con-

siderably higher carbon release potential underlines the critical importance of investigating boreal bogs.

4.5.3 Nutrient treatments

Concerning inorganic nitrogen, H. Zhang et al. (2021) found concentrations of $2.04 \mu\text{g g}^{-1} \text{NO}_3^-$ and $19.10 \mu\text{g g}^{-1} \text{NH}_4^+$ (with variations in the same order as the mean values) in soil extracts from the upper 10 cm of Finnish bogs. Thus their ammonium concentrations were ten times higher than nitrate. On the contrary, Treat et al. (2016) measured approximately three times more nitrate than ammonia, and these were the ratios that were used to estimate the natural ambient concentrations for this experiment. This may be because Treat et al. (2016) report leachate values, and nitrate is more easily leached, while H. Zhang et al. (2021) uses soil extracts; and in fall, nitrate was on the high, ammonium on the low end of ratios within the reported seasonality.

Total dissolved N surpassed the estimated target N₀ concentration by one order of magnitude (see Table 3.2; Note that water nutrient concentrations might be inflated due to the extraction from archive material that had already been frozen and thawed once, potentially leading to cell destruction and leakage of their contents). Additionally, the tap water also contained 1.0 mg L^{-1} nitrate and small amounts of ammonium ($<0.200 \text{ mg L}^{-1}$). Therefore the variation induced by the treatments, especially of nitrate, was lower than the background value. Inorganic N pools vary substantially between sampling sites, times, and depths in other studies (Basiliko et al., 2005; Griffiths and Sebestyen, 2016; H. Zhang et al., 2021) and a different choice of reference may have led to different treatment concentrations. Unfortunately, logistic reasons prevented the quantification of N compounds directly from pre-incubation material. Inorganic N is also the smallest N pool, and organic N should be studied alongside it (Weedon et al., 2012).

The tap water also introduced other nutrients that are presumably scarce in Siikaneva bog, like carbonates and calcium (see A.5). This means that not only a potential N limitation was alleviated for the incubated microbe communities, but also other nutrients. Micronutrients such as Ni, Co, Na and Fe are known factors in methanogenesis (Dolman, 2019, p. 163). Furthermore, the acidic conditions to which bog microbes are adapted were pushed towards neutrality through dilution with slightly alkaline water. However, all samples received the same amount of tap water. This means that the relative variations between treatment groups still provide valuable insights, unless the microbial community deviated substantially from the natural state because the conditions deviated from the acceptable range for some phyla. Altogether, these additional

side effects may have contributed to high within-group variabilities and smaller differences between groups, especially that N treatment variability was small compared to the constant addition with water.

4.5.4 Transferability to the ecosystem scale

Incubations are designed to isolate heterotrophic respiration and observe its drivers in a simplified environment. However, this isolation is also their main shortcoming, and conditions in long-term incubations can deviate quite strongly from real ecosystems (Schädel et al., 2020). For example, the varying transport modes and oxidation that determine real-world methane fluxes are ignored in incubations, and results from laboratory and field flux measurements may be completely uncorrelated (H. Zhang et al., 2021).

Concerning N, incubations remove live sphagnum as an actor in the nutrient cycle. The moss employs several strategies to obtain this essential nutrient, for example, by hosting nitrogen-fixing symbionts in its hyalocytes. Furthermore, vital substrate inputs from plants such as root exudates and litter are missing (Petro et al., 2023). An isolated input of N compounds, as in this study, does not reflect real-world scenarios, where enhanced decomposition by warming or litter input would entail the simultaneous release of other nutrients. It does however more closely resemble inputs by atmospheric decomposition. With increased development of agricultural land in the north that might follow the northward shift of climate zones with global warming, this might become more relevant in the future.

Some climate models predict higher temperatures and less precipitation for northern peatlands (Belyea, 2009, p. 14). This would result in water table drawdown and a deepening of the oxic zone. Another study found strongly increasing winter precipitation in the boreal zone (Poulter et al., 2017). This underlines how local precipitation patterns remain hard to capture in climate models. For a study with a methane focus, a fully anoxic configuration was the most suitable option.

In this study, carbon release as methane from below the water table was more responsive to temperature, but how this translates to fluxes under real-world conditions depends on several factors which might abate methane emissions. For one, methanotrophs are stimulated by rising temperatures even more than methanogens (H. Zhang et al., 2021; Petro et al., 2023), but there also are contrasting results that find oxidation increasingly incapable to compensate for methanogenesis when temperatures exceed 15°C (Windén et al., 2012). On the ecosystem scale, plant diversity and especially the spread of vascular plants may offset methane emissions (Y. Zhang et al., 2023). Incuba-

tions may not directly reflect processes in ecosystems, but aim to isolate single drivers and facilitate process understanding (Schädel et al., 2020). For example, N interactions found in field studies may be caused by a third covariate, like the water table position (Basiliko et al., 2005). Incubations remove such confounders. Despite divergences from natural conditions, longer incubation times result in more stable estimations of temperature sensitivity (Hamdi et al., 2013).

5. Conclusion and outlook

This experiment showed that nitrate and ammonium additions inhibit carbon production from peat samples. Consequently, the results indicate that enhanced N cycling alone does not endanger the peatland carbon sink from the decomposer side.

It further underlined that differentiating between N species is important to predict the response of peat to N addition. This will extend well to studies of ecosystem scale, e.g. because *Sphagnum* mosses prefer ammonium over nitrate (Bobbink et al., 2022).

Warmer temperatures resulted in higher respiration rates, but cumulative carbon release was limited to an apparent labile pool size of about 1.5% of total organic carbon. Differences in carbon mineralization rate, trajectory, and form between the samples from above and below the water reflected the distinct microbial community of dissimilar habitats. Furthermore, nitrogen addenda affected the temperature response of the incubated samples in a multifaceted way that underlines the complexity of decomposition processes even in a simplified environment. The inhibiting effects were potentially caused by a combination of competing metabolic pathways, colimitation, and toxicity. These results also carry relevance beyond northern peatlands. For example, soils in the permafrost domain store large amounts of organic carbon and nitrogen that are vulnerable to thaw, potentially releasing plant-available nitrogen into the peatlands there (Hugelius et al., 2020; Keuper et al., 2012). Enhanced nutrient cycling has also been linked to arctic greening driven by increased soil development in previously sparsely vegetated areas (Doetterl et al., 2022). On the global scale, models of carbon sinks like peatlands need to account for potential N limitation to accurately predict their carbon sequestration potential (Zaehle et al., 2015).

Therefore, future studies should shed more light on the processes behind the coupled N and C cycles in peatlands. They should incorporate N_2O , the third-most impactful greenhouse gas and most direct vector of N impacts on the atmosphere. Measuring it would not only complete the tally of climate impacts of enhanced N cycling, but also provide more insights into the fate of the N addenda. An experimental regression design could help explore effect sizes and potentially nonlinear responses (Gotelli

and Ellison, 2004). To improve the accuracy of the results, it would be advantageous to prepare treatments with water from the site to avoid any unwanted changes, and determine its chemical properties beforehand.

In a future experiment, some headspaces could be artificially enriched with methane to observe a potential uptake by anaerobic methane oxidation (see H. Zhang et al. (2021) and Liebner et al. (2011)). Investigating microbial gene expressions once again in post-incubation material would clarify whether microbes were inhibited or made more efficient by N addenda. The fate of the N addenda could be traced by a repeated analysis of C, N, and ammonium and nitrate.

This would improve understanding of the N impact on the peatland carbon cycle to translate these findings to larger scales and modelling approaches.

Bibliography

- Alekseychik, Pavel, Aino Korrensalo, Ivan Mammarella, Samuli Launiainen, Eeva-Stiina Tuittila, Ilkka Korpela, and Timo Vesala (2021). "Carbon Balance of a Finnish Bog: Temporal Variability and Limiting Factors Based on 6 Years of Eddy-Covariance Data". In: *Biogeosciences* 18.16, pp. 4681–4704. DOI: 10.5194/bg-18-4681-2021.
- Amelung, Wulf, Hans-Peter Blume, Heiner Fleige, Rainer Horn, Ellen Kandeler, Ingrid Kögel-Knabner, Ruben Kretschmar, Karl Stahr, and Berndt-Michael Wilke (2018). "Bodenorganismen und ihr Lebensraum". In: *Scheffer/Schachtschabel Lehrbuch der Bodenkunde*. Berlin, Heidelberg: Springer Berlin Heidelberg, pp. 103–149. DOI: 10.1007/978-3-662-55871-3_4;.
- Arctic Monitoring and Assessment Programme (Name) (2015). *AMAP Assessment 2015: Methane as an Arctic Climate Forcer*. Oslo, p. 139.
- Artz, Rebekka R. E. (2009). "Microbial Community Structure and Carbon Substrate Use in Northern Peatlands". In: *Carbon Cycling in Northern Peatlands*. Ed. by Andrew J. Baird, Lisa R. Belyea, Xavier Comas, A.S. Reeve, and Lee D. Slater. Vol. 184. Geophysical Monograph Series. Washington, D. C.: American Geophysical Union, pp. 111–129. DOI: 10.1029/2008GM000806.
- Baird, Andrew J., Xavier Comas, Lee D. Slater, Lisa R. Belyea, and A. S. Reeve (2009). "Understanding Carbon Cycling in Northern Peatlands: Recent Developments and Future Prospects". In: *Carbon Cycling in Northern Peatlands*. Ed. by Andrew J. Baird, Lisa R. Belyea, Xavier Comas, A.S. Reeve, and Lee D. Slater. Vol. 184. Geophysical Monograph Series. Washington, D. C.: American Geophysical Union, pp. 1–3. DOI: 10.1029/2008GM000875.
- Basiliko, Nathan, Tim R. Moore, Peter M. Lafleur, and Nigel T. Roulet (2005). "Seasonal and Inter-Annual Decomposition, Microbial Biomass, and Nitrogen Dynamics in a Canadian Bog". In: *Soil Science* 170.11, pp. 902–912. DOI: 10.1097/01.ss.0000196765.59412.14.
- Baysinger, Mackenzie Rae, Susanne Liebner, Jens Strauss, Sizhong Yang, Katharina Jentsch, Alexander Bartholomäus, and Claire Clark Treat (2024). *Anaerobic Respiration*

- tion and Temperature Response along a Boreal Hydrological Transect on a Slope from Upland Forest to Peatland*. URL: <https://essopenarchive.org/users/745456/articles/717482-anaerobic-respiration-and-temperature-response-along-a-boreal-hydrological-transect-on-a-slope-from-upland-forest-to-peatland?commit=7c32e48678bf31e690d221216c1017b0c5a21c1d> (visited on 03/12/2024). preprint.
- Belyea, Lisa R. (2009). "Nonlinear Dynamics of Peatlands and Potential Feedbacks on the Climate System". In: *Carbon Cycling in Northern Peatlands*. Ed. by Andrew J. Baird, Lisa R. Belyea, Xavier Comas, A.S. Reeve, and Lee D. Slater. Geophysical Monograph Series 184. Washington, D. C.: American Geophysical Union, pp. 5–18. DOI: 10.1029/2008GM000829.
- Bobbink, Roland, Christin Loran, and Hilde Tomassen (2022). *Review and Revision of Empirical Critical Loads of Nitrogen for Europe*. German Environmental Agency.
- Bodelier, Paul LE and Anne K Steenberg (2014). "Interactions between Methane and the Nitrogen Cycle in Light of Climate Change". In: *Current Opinion in Environmental Sustainability*. SI: System Dynamics and Sustainability 9–10, pp. 26–36. DOI: 10.1016/j.cosust.2014.07.004.
- Bragazza, Luca, Alexandre Buttler, Andy Siegenthaler, and Edward A. D. Mitchell (2009). "Plant Litter Decomposition and Nutrient Release in Peatlands". In: *Carbon Cycling in Northern Peatlands*. Ed. by Andrew J. Baird, Lisa R. Belyea, Xavier Comas, A.S. Reeve, and Lee D. Slater. Vol. 184. Geophysical Monograph Series. Washington, D. C.: American Geophysical Union, pp. 99–110. DOI: 10.1029/2008GM000815.
- Bragazza, Luca, Chris Freeman, Timothy Jones, Håkan Rydin, Juul Limpens, Nathalie Fenner, Tim Ellis, Renato Gerdol, Michal Hájek, Tomáš Hájek, Paola Iacumin, Lado Kutnar, Teemu Tahvanainen, and Hannah Toberman (2006). "Atmospheric Nitrogen Deposition Promotes Carbon Loss from Peat Bogs". In: *Proceedings of the National Academy of Sciences* 103.51, pp. 19386–19389. DOI: 10.1073/pnas.0606629104.
- Breeuwer, Angela, Monique Heijmans, Bjorn J. M. Robroek, Juul Limpens, and Frank Berendse (2008). "The Effect of Increased Temperature and Nitrogen Deposition on Decomposition in Bogs". In: *Oikos* 117.8, pp. 1258–1268. DOI: 10.1111/j.0030-1299.2008.16518.x.
- Burkholder, J.B., S.P. Sander, J. Abbatt, J.R. Barker, C. Cappa, J.D. Crouse, T.S. Dibble, R.E. Huie, C.E. Kolb, M.J. Kurylo, V.L. Orkin, C.J. Percival, D.M. Wilmouth, and P.H. Wine (2019). *Chemical Kinetics and Photochemical Data for Use in Atmospheric Studies, Evaluation No. 19*. JPL Publication 19-5. Pasadena: Jet Propulsion Laboratory.
- Carfrae, J.A., L.J. Sheppard, J.A. Raven, I.D. Leith, and A. Crossley (2007). "Potassium and Phosphorus Additions Modify the Response of Sphagnum Capillifolium Grow-

- ing on a Scottish Ombrotrophic Bog to Enhanced Nitrogen Deposition". In: *Applied Geochemistry* 22.6, pp. 1111–1121. DOI: 10.1016/j.apgeochem.2007.03.002.
- Chen, Leiyi, Li Liu, Chao Mao, Shuqi Qin, Jun Wang, Futing Liu, Sergey Blagodatsky, Guibiao Yang, Qiwen Zhang, Dianye Zhang, Jianchun Yu, and Yuanhe Yang (2018). "Nitrogen Availability Regulates Topsoil Carbon Dynamics after Permafrost Thaw by Altering Microbial Metabolic Efficiency". In: *Nature Communications* 9.1, p. 3951. DOI: 10.1038/s41467-018-06232-y.
- Chen, Ye, Jay J. Cheng, and Kurt S. Creamer (2008). "Inhibition of Anaerobic Digestion Process: A Review". In: *Bioresource Technology* 99.10, pp. 4044–4064. DOI: 10.1016/j.biortech.2007.01.057.
- Currey, Pauline M., David Johnson, Lucy J. Sheppard, Ian D. Leith, Hannah Toberman, René Van Der Wal, Lorna A. Dawson, and Rebekka R. E. Artz (2009). "Turnover of Labile and Recalcitrant Soil Carbon Differ in Response to Nitrate and Ammonium Deposition in an Ombrotrophic Peatland: Enzyme Response to N in Peatlands". In: *Global Change Biology* 16.8, pp. 2307–2321. DOI: 10.1111/j.1365-2486.2009.02082.x.
- Dean, Joshua F., Jack J. Middelburg, Thomas Röckmann, Rien Aerts, Luke G. Blauw, Matthias Egger, Mike S. M. Jetten, Anniek E. E. De Jong, Ove H. Meisel, Olivia RasiGRAF, Caroline P. Slomp, Michiel H. In'T Zandt, and A. J. Dolman (2018). "Methane Feedbacks to the Global Climate System in a Warmer World". In: *Reviews of Geophysics* 56.1, pp. 207–250. DOI: 10.1002/2017RG000559.
- DeLaune, R.D., K.R. Reddy, C.J. Richardson, and J.P. Megonigal, eds. (2013). *Methods in Biogeochemistry of Wetlands*. SSSA Book Series. Madison, WI, USA: American Society of Agronomy and Soil Science Society of America. DOI: 10.2136/sssabookser10.
- Dierßen, Klaus and Barbara Dierßen (2001). *Moore. Ökosysteme Mitteleuropas Aus Geobotanischer Sicht 2*. Stuttgart (Hohenheim): Ulmer.
- Doetterl, Sebastian, Jake Alexander, Simone Fior, Aline Frossard, Cara Magnabosco, Marijn Broek, and Kristine Bakke Westergaard (2022). "Will Accelerated Soil Development Be a Driver of Arctic Greening in the Late 21st Century?" In: *Journal of Plant Nutrition and Soil Science* 185.1, pp. 19–23. DOI: 10.1002/jp1n.202100334.
- Dolman, A. J. (2019). *Biogeochemical Cycles and Climate*. First edition. Oxford, United Kingdom: Oxford University Press. 251 pp.
- EMEP (2023). *Transboundary Particulate Matter, Photo-Oxidant, Acidifying and Eutrophying Components*. 1/2023. Co-operative programme for monitoring and evaluation of the long-range transmission of air pollutants in Europe.
- Energie und Wasser Potsdam GmbH (2022). *Aktuelle Trinkwasseranalyse*.

- Fowler, David, Mhairi Coyle, Ute Skiba, Mark A. Sutton, J. Neil Cape, Stefan Reis, Lucy J. Sheppard, Alan Jenkins, Bruna Grizzetti, James N. Galloway, Peter Vitousek, Allison Leach, Alexander F. Bouwman, Klaus Butterbach-Bahl, Frank Dentener, David Stevenson, Marcus Amann, and Maren Voss (2013). "The Global Nitrogen Cycle in the Twenty-First Century". In: *Philosophical Transactions of the Royal Society B: Biological Sciences* 368.1621, p. 20130164. DOI: 10.1098/rstb.2013.0164.
- Francez, André-Jean, Gilles Pinay, Nathalie Josselin, and Berwyn L. Williams (2011). "Denitrification Triggered by Nitrogen Addition in Sphagnum Magellanicum Peat". In: *Biogeochemistry* 106.3, pp. 435–441. DOI: 10.1007/s10533-010-9523-5.
- GCTE-NEWS, L. Rustad, J. Campbell, G. Marion, R. Norby, M. Mitchell, A. Hartley, J. Cornelissen, and J. Gurevitch (2001). "A Meta-Analysis of the Response of Soil Respiration, Net Nitrogen Mineralization, and Aboveground Plant Growth to Experimental Ecosystem Warming". In: *Oecologia* 126.4, pp. 543–562. DOI: 10.1007/s004420000544.
- Glaser, Paul H. and J. P. Chanton (2009). "Methane Accumulation and Release from Deep Peat: Measurements, Conceptual Models, and Biogeochemical Significance". In: *Carbon Cycling in Northern Peatlands*. Ed. by Andrew J. Baird, Lisa R. Belyea, Xavier Comas, A.S. Reeve, and Lee D. Slater. Geophysical Monograph Series 184. Washington, D. C.: American Geophysical Union, pp. 145–158.
- Golde, Lion (2023). "Classification of a High Latitude Bog Using Multispectral Drone Imagery". Berlin.
- Gotelli, Nicholas J. and Aaron M. Ellison (2004). "A Primer of Ecological Statistics". In: Griffiths, Natalie A. and Stephen D. Sebestyen (2016). "Dynamic Vertical Profiles of Peat Porewater Chemistry in a Northern Peatland". In: *Wetlands* 36.6, pp. 1119–1130. DOI: 10.1007/s13157-016-0829-5.
- Gupta, Varun, Kurt A. Smemo, Joseph B. Yavitt, David Fowle, Brian Branfireun, and Nathan Basiliko (2013). "Stable Isotopes Reveal Widespread Anaerobic Methane Oxidation Across Latitude and Peatland Type". In: *Environmental Science & Technology*, p. 130717064455005. DOI: 10.1021/es400484t.
- Hamdi, Salwa, Fernando Moyano, Saidou Sall, Martial Bernoux, and Tiphaine Chevalier (2013). "Synthesis Analysis of the Temperature Sensitivity of Soil Respiration from Laboratory Studies in Relation to Incubation Methods and Soil Conditions". In: *Soil Biology and Biochemistry* 58, pp. 115–126. DOI: 10.1016/j.soilbio.2012.11.012.
- Heijmans, Monique M.P.D., Dmitri Mauquoy, Bas Van Geel, and Frank Berendse (2008). "Long-Term Effects of Climate Change on Vegetation and Carbon Dynamics in Peat Bogs". In: *Journal of Vegetation Science* 19.3, pp. 307–320. DOI: 10.3170/2008-8-18368.

- Hettelingh, J.P., M. Posch, and J. Slootweg (2017). "European Critical Loads: Database, Biodiversity and Ecosystems at Risk". In: DOI: 10.21945/RIVM-2017-0155.
- Hugelius, Gustaf, Julie Loisel, Sarah Chadburn, Robert B. Jackson, Miriam Jones, Glen MacDonald, Maija Marushchak, David Olefeldt, Maara Packalen, Matthias B. Siewert, Claire Treat, Merritt Turetsky, Carolina Voigt, and Zicheng Yu (2020). "Large Stocks of Peatland Carbon and Nitrogen Are Vulnerable to Permafrost Thaw". In: *Proceedings of the National Academy of Sciences* 117.34, pp. 20438–20446. DOI: 10.1073/pnas.1916387117.
- Intergovernmental Panel On Climate Change (2023). *Climate Change 2021 – The Physical Science Basis: Working Group I Contribution to the Sixth Assessment Report of the Intergovernmental Panel on Climate Change*. 1st ed. Cambridge University Press. DOI: 10.1017/9781009157896.
- Iversen, Colleen M., John Latimer, Deanne J. Brice, Joanne Childs, Holly M. Vander Stel, Camille E. Defrenne, Jake Graham, Natalie A. Griffiths, Avni Malhotra, Richard J. Norby, Keith C. Oleheiser, Jana R. Phillips, Verity G. Salmon, Stephen D. Sebestyen, Xiaojuan Yang, and Paul J. Hanson (2023). "Whole-Ecosystem Warming Increases Plant-Available Nitrogen and Phosphorus in an Ombrotrophic Bog". In: *Ecosystems* 26.1, pp. 86–113. DOI: 10.1007/s10021-022-00744-x.
- Jackson, Robert B., Kate Lajtha, Susan E. Crow, Gustaf Hugelius, Marc G. Kramer, and Gervasio Piñeiro (2017). "The Ecology of Soil Carbon: Pools, Vulnerabilities, and Biotic and Abiotic Controls". In: *Annual Review of Ecology, Evolution, and Systematics* 48.1, pp. 419–445. DOI: 10.1146/annurev-ecolsys-112414-054234.
- Jentzsch, Katharina, Elisa Männistö, Maija E. Marushchak, Aino Korrensalo, Lona Van Delden, Eeva-Stiina Tuittila, Christian Knoblauch, and Claire C. Treat (2024). *Seasonal Controls on Methane Flux Components in a Boreal Peatland – Combining Plant Removal and Stable Isotope Analyses*. DOI: 10.5194/egusphere-2023-3098. preprint.
- Juutinen, Sari, Tim R. Moore, Jill L. Bubier, Sini Arnkil, Elyn Humphreys, Brenden Marincak, Cameron Roy, and Tuula Larmola (2018). "Long-Term Nutrient Addition Increased CH₄ Emission from a Bog through Direct and Indirect Effects". In: *Scientific Reports* 8.1, p. 3838. DOI: 10.1038/s41598-018-22210-2.
- Keuper, Frida, Peter M. Bodegom, Ellen Dorrepaal, James T. Weedon, Jurgen Hal, Richard S. P. Logtestijn, and Rien Aerts (2012). "A Frozen Feast: Thawing Permafrost Increases Plant-Available Nitrogen in Subarctic Peatlands". In: *Global Change Biology* 18.6, pp. 1998–2007. DOI: 10.1111/j.1365-2486.2012.02663.x.
- Kim, Sang Yoon, Annelies J. Veraart, Marion Meima-Franke, and Paul L. E. Bodelier (2015). "Combined Effects of Carbon, Nitrogen and Phosphorus on CH₄ Production

- and Denitrification in Wetland Sediments". In: *Geoderma* 259–260, pp. 354–361. DOI: 10.1016/j.geoderma.2015.03.015.
- Knoblauch, Christian, Christian Beer, Alexander Sosnin, Dirk Wagner, and Eva-Maria Pfeiffer (2013). "Predicting Long-Term Carbon Mineralization and Trace Gas Production from Thawing Permafrost of Northeast Siberia". In: *Global Change Biology* 19.4, pp. 1160–1172. DOI: 10.1111/gcb.12116.
- Korrensalo, Aino, Laura Kettunen, Raija Laiho, Pavel Alekseychik, Timo Vesala, Ivan Mammarella, and Eeva-Stiina Tuittila (2018). "Boreal Bog Plant Communities along a Water Table Gradient Differ in Their Standing Biomass but Not Their Biomass Production". In: *Journal of Vegetation Science* 29.2. Ed. by Stephen Roxburgh, pp. 136–146. DOI: 10.1111/jvs.12602.
- Laurent, Mélissa, Matthias Fuchs, Tanja Herbst, Alexandra Runge, Susanne Liebner, and Claire C. Treat (2023). "Relationships between Greenhouse Gas Production and Landscape Position during Short-Term Permafrost Thaw under Anaerobic Conditions in the Lena Delta". In: *Biogeosciences* 20.11, pp. 2049–2064. DOI: 10.5194/bg-20-2049-2023.
- Lavoie, M., M. C. Mack, and E. A. G. Schuur (2011). "Effects of Elevated Nitrogen and Temperature on Carbon and Nitrogen Dynamics in Alaskan Arctic and Boreal Soils". In: *Journal of Geophysical Research* 116.G3, G03013. DOI: 10.1029/2010JG001629.
- Liebner, Susanne, Josef Zeyer, Dirk Wagner, Carsten Schubert, Eva-Maria Pfeiffer, and Christian Knoblauch (2011). "Methane Oxidation Associated with Submerged Brown Mosses Reduces Methane Emissions from Siberian Polygonal Tundra: Moss-associated Methane Oxidation". In: *Journal of Ecology* 99.4, pp. 914–922. DOI: 10.1111/j.1365-2745.2011.01823.x.
- Liu, Lingli and Tara L. Greaver (2009). "A Review of Nitrogen Enrichment Effects on Three Biogenic GHGs: The CO₂ Sink May Be Largely Offset by Stimulated N₂O and CH₄ Emission". In: *Ecology Letters* 12.10, pp. 1103–1117. DOI: 10.1111/j.1461-0248.2009.01351.x.
- Martí, M., M.B. Nilsson, Å. Danielsson, P-E. Lindgren, and B.H. Svensson (2019). "Strong Long-Term Interactive Effects of Warming and Enhanced Nitrogen and Sulphur Deposition on the Abundance of Active Methanogens in a Boreal Oligotrophic Mire". In: *Mires and Peat* 24, pp. 1–14. DOI: 10.19189/MaP.2019.OMB.398.
- Mathijssen, Paul J.H., Minna Väiliranta, Aino Korrensalo, Pavel Alekseychik, Timo Vesala, Janne Rinne, and Eeva-Stiina Tuittila (2016). "Reconstruction of Holocene Carbon Dynamics in a Large Boreal Peatland Complex, Southern Finland". In: *Quaternary Science Reviews* 142, pp. 1–15. DOI: 10.1016/j.quascirev.2016.04.013.

- Müller, Jurek and Fortunat Joos (2021). "Committed and Projected Future Changes in Global Peatlands – Continued Transient Model Simulations since the Last Glacial Maximum". In: *Biogeosciences* 18.12, pp. 3657–3687. DOI: 10.5194/bg-18-3657-2021.
- Nazaries, Loïc, J. Colin Murrell, Pete Millard, Liz Baggs, and Brajesh K. Singh (2013). "Methane, Microbes and Models: Fundamental Understanding of the Soil Methane Cycle for Future Predictions". In: *Environmental Microbiology* 15.9, pp. 2395–2417. DOI: 10.1111/1462-2920.12149.
- Neubauer, Scott C. and J. Patrick Megonigal (2015). "Moving Beyond Global Warming Potentials to Quantify the Climatic Role of Ecosystems". In: *Ecosystems* 18.6, pp. 1000–1013. DOI: 10.1007/s10021-015-9879-4.
- Nilsson, M. and M. Öquist (2009). "Partitioning Litter Mass Loss into Carbon Dioxide and Methane in Peatland Ecosystems". In: *Carbon Cycling in Northern Peatlands*. Ed. by Andrew J. Baird, Lisa R. Belyea, Xavier Comas, A.S. Reeve, and Lee D. Slater. Geophysical Monograph Series 184. Washington, D. C.: American Geophysical Union, pp. 131–144. DOI: 10.1029/2008GM000819.
- Peltoniemi, Krista, Raija Laiho, Heli Juottonen, Levente Bodrossy, Dana K. Kell, Kari Minkkinen, Päivi Mäkiranta, Lauri Mehtätalo, Timo Penttilä, Henri M. P. Siljanen, Eeva-Stiina Tuittila, Tero Tuomivirta, and Hannu Fritze (2016). "Responses of Methanogenic and Methanotrophic Communities to Warming in Varying Moisture Regimes of Two Boreal Fens". In: *Soil Biology and Biochemistry* 97, pp. 144–156. DOI: 10.1016/j.soilbio.2016.03.007.
- Petro, Caitlin, Alyssa A. Carrell, Rachel M. Wilson, Katherine Duchesneau, Sekou Noble-Kuchera, Tianze Song, Colleen M. Iversen, Joanne Childs, Geoff Schwaner, Jeffrey P. Chanton, Richard J. Norby, Paul J. Hanson, Jennifer B. Glass, David J. Weston, and Joel E. Kostka (2023). "Climate Drivers Alter Nitrogen Availability in Surface Peat and Decouple N_2 Fixation from CH_4 Oxidation in the *Sphagnum* Moss Microbiome". In: *Global Change Biology* 29.11, pp. 3159–3176. DOI: 10.1111/gcb.16651.
- Poulter, Benjamin et al. (2017). "Global Wetland Contribution to 2000–2012 Atmospheric Methane Growth Rate Dynamics". In: *Environmental Research Letters* 12.9, p. 094013. DOI: 10.1088/1748-9326/aa8391.
- R Core Team (2023). *R: A Language and Environment for Statistical Computing*. manual. Vienna, Austria: R Foundation for Statistical Computing.
- Raghoebarsing, Ashna A., Alfons J. P. Smolders, Markus C. Schmid, W. Irene C. Rijpstra, Mieke Wolters-Arts, Jan Derksen, Mike S. M. Jetten, Stefan Schouten, Jaap S. Sinninghe Damsté, Leon P. M. Lamers, Jan G. M. Roelofs, Huub J. M. Op Den Camp,

- and Marc Strous (2005). "Methanotrophic Symbionts Provide Carbon for Photosynthesis in Peat Bogs". In: *Nature* 436.7054, pp. 1153–1156. DOI: 10.1038/nature03802.
- Rankin, Tracy E., Nigel T. Roulet, and Tim R. Moore (2022). "Controls on Autotrophic and Heterotrophic Respiration in an Ombrotrophic Bog". In: *Biogeosciences* 19.13, pp. 3285–3303. DOI: 10.5194/bg-19-3285-2022.
- Reddy, K. Ramesh, Ronald D. DeLaune, and Patrick W. Inglett (2023). *Biogeochemistry of Wetlands: Science and Applications*. 2nd ed. Boca Raton: CRC Press. DOI: 10.1201/9780429155833.
- Robertson, G. P., David C. Coleman, Caroline S. Bledsoe, and Phillip Sollins, eds. (1999). *Standard Soil Methods for Long-Term Ecological Research*. Long-Term Ecological Research Network Series 2. New York: Oxford University Press. 462 pp.
- Rogelj, Joeri and Robin D. Lamboll (2024). "Substantial Reductions in Non-CO2 Greenhouse Gas Emissions Reductions Implied by IPCC Estimates of the Remaining Carbon Budget". In: *Communications Earth & Environment* 5.1 (1), pp. 1–5. DOI: 10.1038/s43247-023-01168-8.
- Salmon, Verity G., Patrick Soucy, Marguerite Mauritz, Gerardo Celis, Susan M. Natali, Michelle C. Mack, and Edward A. G. Schuur (2016). "Nitrogen Availability Increases in a Tundra Ecosystem during Five Years of Experimental Permafrost Thaw". In: *Global Change Biology* 22.5, pp. 1927–1941. DOI: 10.1111/gcb.13204. pmid: 26718892.
- Sander, Rolf (2023). "Compilation of Henry's Law Constants (Version 5.0.0) for Water as Solvent". In: *Atmospheric Chemistry and Physics* 23.19, pp. 10901–12440. DOI: 10.5194/acp-23-10901-2023.
- Schädel, Christina, Jeffrey Beem-Miller, Mina Aziz Rad, Susan E. Crow, Caitlin E. Hicks Pries, Jessica Ernakovich, Alison M. Hoyt, Alain Plante, Shane Stoner, Claire C. Treat, and Carlos A. Sierra (2020). "Decomposability of Soil Organic Matter over Time: The Soil Incubation Database (SIDb, Version 1.0) and Guidance for Incubation Procedures". In: *Earth System Science Data* 12.3, pp. 1511–1524. DOI: 10.5194/essd-12-1511-2020.
- Schimel, J and Michael N. Weintraub (2003). "The Implications of Exoenzyme Activity on Microbial Carbon and Nitrogen Limitation in Soil: A Theoretical Model". In: *Soil Biology and Biochemistry* 35.4, pp. 549–563. DOI: 10.1016/S0038-0717(03)00015-4.
- Sheppard, L. J., I. D. Leith, S. R. Leeson, N. van Dijk, C. Field, and P. Levy (2013). "Fate of N in a Peatland, Whim Bog: Immobilisation in the Vegetation and Peat, Leakage into Pore Water and Losses as N₂O Depend on the Form of N". In: *Biogeosciences* 10.1, pp. 149–160. DOI: 10.5194/bg-10-149-2013.

- Sierra, C. A., M. Müller, and S. E. Trumbore (2012). "Models of Soil Organic Matter Decomposition: The SoilR Package, Version 1.0". In: *Geoscientific Model Development* 5.4, pp. 1045–1060. DOI: 10.5194/gmd-5-1045-2012.
- Soetaert, Karline and Thomas Petzoldt (2010). "Inverse Modelling, Sensitivity and Monte Carlo Analysis in R Using Package FME". In: *Journal of Statistical Software* 33.3. DOI: 10.18637/jss.v033.i03.
- Treat, Claire C., Susan M. Natali, Jessica Ernakovich, Colleen M. Iversen, Massimo Lupascu, Anthony David McGuire, Richard J. Norby, Taniya Roy Chowdhury, Andreas Richter, Hana Šantrůčková, Christina Schädel, Edward A. G. Schuur, Victoria L. Sloan, Merritt R. Turetsky, and Mark P. Waldrop (2015). "A pan-Arctic Synthesis of CH₄ and CO₂ Production from Anoxic Soil Incubations". In: *Global Change Biology* 21.7, pp. 2787–2803. DOI: 10.1111/gcb.12875.
- Treat, Claire C., Wilfred M Wollheim, Ruth K Varner, and William B Bowden (2016). "Longer Thaw Seasons Increase Nitrogen Availability for Leaching during Fall in Tundra Soils". In: *Environmental Research Letters* 11.6, p. 064013. DOI: 10.1088/1748-9326/11/6/064013.
- Van Groenigen, Kees Jan, Craig W. Osenberg, and Bruce A. Hungate (2011). "Increased Soil Emissions of Potent Greenhouse Gases under Increased Atmospheric CO₂". In: *Nature* 475.7355, pp. 214–216. DOI: 10.1038/nature10176.
- Vuorenmaa, Jussi, Algirdas Augustaitis, Burkhard Beudert, Nicholas Clarke, Heleen A.de Wit, Thomas Dirnböck, Jane Frey, Martin Forsius, Iveta Indriksone, Sirpa Kleemola, Johannes Kobler, Pavel Krám, Antti-Jussi Lindroos, Lars Lundin, Tuija Ruoho-Airola, Liisa Ukonmaanaho, and Milan Váňa (2017). "Long-Term Sulphate and Inorganic Nitrogen Mass Balance Budgets in European ICP Integrated Monitoring Catchments (1990–2012)". In: *Ecological Indicators* 76, pp. 15–29. DOI: 10.1016/j.ecolind.2016.12.040.
- Weedon, James T., George A. Kowalchuk, Rien Aerts, Jurgen van Hal, Richard van Logtestijn, Neslihan Taş, Wilfred F. M. Röling, and Peter M. van Bodegom (2012). "Summer Warming Accelerates Sub-Arctic Peatland Nitrogen Cycling without Changing Enzyme Pools or Microbial Community Structure". In: *Global Change Biology* 18.1, pp. 138–150. DOI: 10.1111/j.1365-2486.2011.02548.x.
- Weedon, James T., Rien Aerts, George A. Kowalchuk, Richard Van Logtestijn, Dave Andringa, and Peter M. Van Bodegom (2013). "Temperature Sensitivity of Peatland C and N Cycling: Does Substrate Supply Play a Role?" In: *Soil Biology and Biochemistry* 61, pp. 109–120. DOI: 10.1016/j.soilbio.2013.02.019.

- Wickham, Hadley, Mara Averick, Jennifer Bryan, Winston Chang, Lucy McGowan, Romain François, Garrett Grolemond, Alex Hayes, Lionel Henry, Jim Hester, Max Kuhn, Thomas Pedersen, Evan Miller, Stephan Bache, Kirill Müller, Jeroen Ooms, David Robinson, Dana Seidel, Vitalie Spinu, Kohske Takahashi, Davis Vaughan, Claus Wilke, Kara Woo, and Hiroaki Yutani (2019). "Welcome to the Tidyverse". In: *Journal of Open Source Software* 4.43, p. 1686. DOI: 10.21105/joss.01686.
- Wieder, R. Kelman, Dale H. Vitt, Melanie A. Vile, Jeremy A. Graham, Jeremy A. Hartsock, Hope Fillingim, Melissa House, James C. Quinn, Kimberli D. Scott, Meaghan Petix, and Kelly J. McMillen (2019). "Experimental Nitrogen Addition Alters Structure and Function of a Boreal Bog: Critical Load and Thresholds Revealed". In: *Ecological Monographs* 89.3, e01371. DOI: 10.1002/ecm.1371.
- Wilmoth, Jared L., Jeffra K. Schaefer, Danielle R. Schlesinger, Spencer W. Roth, Patrick G. Hatcher, Julie K. Shoemaker, and Xinning Zhang (2021). "The Role of Oxygen in Stimulating Methane Production in Wetlands". In: *Global Change Biology* 27.22, pp. 5831–5847. DOI: 10.1111/gcb.15831.
- Windén, Julia F. van, Gert-Jan Reichart, Niall P. McNamara, Albert Benthien, and Jaap S. Sinninghe Damsté (2012). "Temperature-Induced Increase in Methane Release from Peat Bogs: A Mesocosm Experiment". In: *PLOS ONE* 7.6, e39614. DOI: 10.1371/journal.pone.0039614.
- Wu, Jianghua and Nigel T. Roulet (2014). "Climate Change Reduces the Capacity of Northern Peatlands to Absorb the Atmospheric Carbon Dioxide: The Different Responses of Bogs and Fens". In: *Global Biogeochemical Cycles* 28.10, pp. 1005–1024. DOI: 10.1002/2014GB004845.
- Yu, Zicheng (2011). "Holocene Carbon Flux Histories of the World's Peatlands: Global Carbon-Cycle Implications". In: *The Holocene* 21.5, pp. 761–774. DOI: 10.1177/0959683610386982.
- Yu, Zicheng, David W. Beilman, and Miriam C. Jones (2009). "Sensitivity of Northern Peatland Carbon Dynamics to Holocene Climate Change". In: *Carbon Cycling in Northern Peatlands*. Ed. by Andrew J. Baird, Lisa R. Belyea, Xavier Comas, A.S. Reeve, and Lee D. Slater. Geophysical Monograph Series 184. Washington, D. C.: American Geophysical Union, pp. 55–69. DOI: 10.1029/2008GM000822.
- Zaehle, Sönke (2013). "Terrestrial Nitrogen–Carbon Cycle Interactions at the Global Scale". In: *Philosophical Transactions of the Royal Society B: Biological Sciences* 368.1621, p. 20130125. DOI: 10.1098/rstb.2013.0125.
- Zaehle, Sönke, Chris D. Jones, Benjamin Houlton, Jean-Francois Lamarque, and Eddy Robertson (2015). "Nitrogen Availability Reduces CMIP5 Projections of Twenty-First-

- Century Land Carbon Uptake". In: *Journal of Climate* 28.6, pp. 2494–2511. DOI: 10.1175/JCLI-D-13-00776.1.
- Zhang, Hui, Eeva-Stiina Tuittila, Aino Korrensalo, Anna M. Laine, Salli Uljas, Nina Welti, Johanna Kerttula, Marja Maljanen, David Elliott, Timo Vesala, and Annalea Lohila (2021). "Methane Production and Oxidation Potentials along a Fen-bog Gradient from Southern Boreal to Subarctic Peatlands in Finland". In: *Global Change Biology* 27.18, pp. 4449–4464. DOI: 10.1111/gcb.15740.
- Zhang, Yifei, Changchun Song, Xianwei Wang, Ning Chen, Guobao Ma, Hao Zhang, Xiaofeng Cheng, and Dongyao Sun (2023). "How Climate Warming and Plant Diversity Affect Carbon Greenhouse Gas Emissions from Boreal Peatlands: Evidence from a Mesocosm Study". In: *Journal of Cleaner Production* 404, p. 136905. DOI: 10.1016/j.jclepro.2023.136905.

Acknowledgements

I'd like to thank Claire Treat who opened the doors to higher latitudes for me. Thank you for reminding me not to forget the big picture - and thank you, Karin Potthast, for sharpening my vision for the small details. And Mack Baysinger - you truly planted an enthusiasm for moss in me, and without you, these incubation vials would still sit empty in the shelves.

Antje Eulenburg, Justin Lindemann and Dan Warner have my eternal admiration and gratitude for managing labs full of rebellious instruments and still finding generous amounts of time to help a confused student.

I'm also grateful to my incubation big sister Madina Dolle who taught me everything I know about sampling, and all the emotional and scientific support. Emergency headspace sampler surgeries were so much more fun with you. I'm thankful to Jonas Vollmer and Sarah Wocheslander who lent me their hands when mine weren't enough. Many thanks to Susanne Liebner and her lab at GeoForschungsZentrum for squeezing my humble samples into your microbial assays, and for Oliver Burckhardt for lending the anaerobic workstation and his patient advice.

Thanks to the other incubation and permafrost people for discussions, support, and coffee breaks. Staying at AWI Potsdam was truly a transformative experience, as finding a community of wonderful science friends was really inspiring.

Declaration of originality / Eigenständigkeitserklärung

1. Hiermit versichere ich, dass ich die vorliegende Arbeit selbstständig verfasst und keine anderen als die angegebenen Quellen und Hilfsmittel benutzt habe. Ich trage die Verantwortung für die Qualität des Textes sowie die Auswahl aller Inhalte und habe sichergestellt, dass Informationen und Argumente mit geeigneten wissenschaftlichen Quellen belegt bzw. gestützt werden. Die aus fremden oder auch eigenen, älteren Quellen wörtlich oder sinngemäß übernommenen Textstellen, Gedankengänge, Konzepte, Grafiken etc. in meinen Ausführungen habe ich als solche eindeutig gekennzeichnet und mit vollständigen Verweisen auf die jeweilige Quelle versehen. Alle weiteren Inhalte dieser Arbeit ohne entsprechende Verweise stammen im urheberrechtlichen Sinn von mir.
2. Ich weiß, dass meine Eigenständigkeitserklärung sich auch auf nicht zitierfähige, generierende KI-Anwendungen (nachfolgend „generierende KI“) bezieht. Mir ist bewusst, dass die Verwendung von generierender KI unzulässig ist, sofern nicht deren Nutzung von der prüfenden Person ausdrücklich freigegeben wurde (Freigabeerklärung). Sofern eine Zulassung als Hilfsmittel erfolgt ist, versichere ich, dass ich mich generierender KI lediglich als Hilfsmittel bedient habe und in der vorliegenden Arbeit mein gestalterischer Einfluss deutlich überwiegt. Ich verantworte die Übernahme der von mir verwendeten maschinell generierten Passagen in meiner Arbeit vollumfänglich selbst. Für den Fall der Freigabe der Verwendung von generierender KI für die Erstellung der vorliegenden Arbeit wird eine Verwendung in einem gesonderten Anhang meiner Arbeit kenntlich gemacht. Dieser Anhang enthält eine Angabe oder eine detaillierte Dokumentation über die Verwendung generierender KI gemäß den Vorgaben in der Freigabeerklärung der prüfenden Person. Die Details zum Gebrauch generierender KI bei der Erstellung der vorliegenden Arbeit inklusive Art, Ziel und Umfang der Verwendung sowie die Art der Nachweispflicht habe ich der Freigabeerklärung der prüfenden Person entnommen.
3. Ich versichere des Weiteren, dass die vorliegende Arbeit bisher weder im In- noch im Ausland in gleicher oder ähnlicher Form einer anderen Prüfungsbehörde vorgelegt wurde oder in deutscher oder einer anderen Sprache als Veröffentlichung erschienen ist.
4. Mir ist bekannt, dass ein Verstoß gegen die vorbenannten Punkte prüfungsrechtliche Konsequenzen haben und insbesondere dazu führen kann, dass meine Prüfungsleistung als Täuschung und damit als mit „nicht bestanden“ bewertet werden kann. Bei mehrfachem oder schwerwiegendem Täuschungsversuch kann ich befristet oder sogar dauerhaft von der Erbringung weiterer Prüfungsleistungen in meinem Studiengang ausgeschlossen werden.

Jena, April 9, 2024

Name

A. Appendix

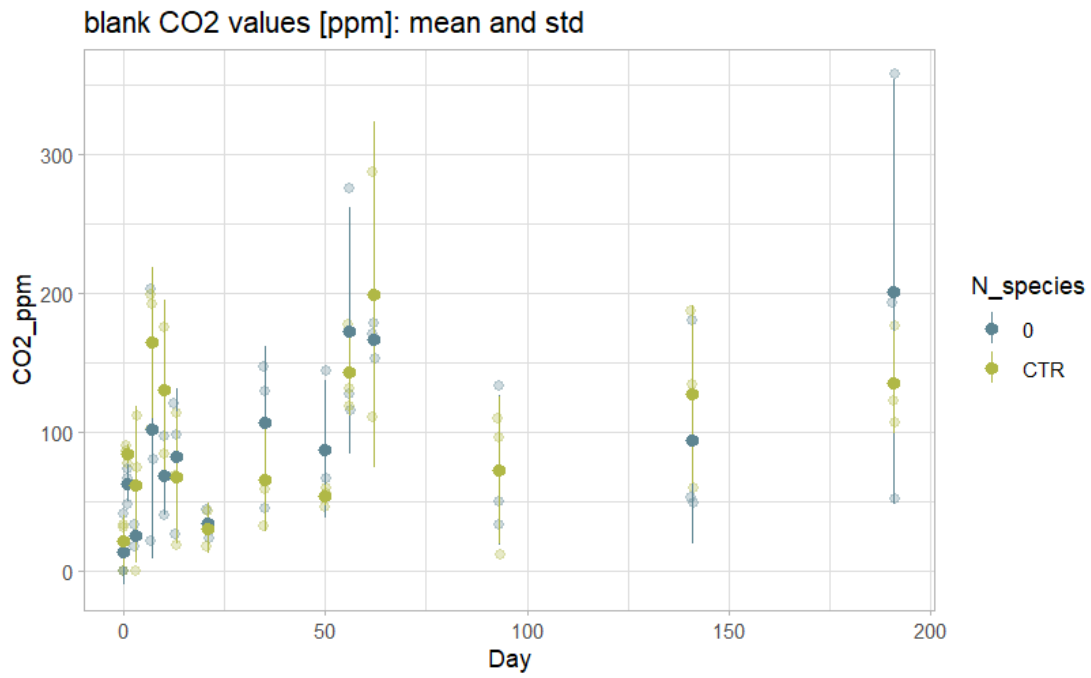
A.1 GC instrument details

The headspace sampler heats the vial to 75 °C and extracts gas through a needle, which is then transferred at 150°C to the main instrument. The GC itself operates at 35°C.

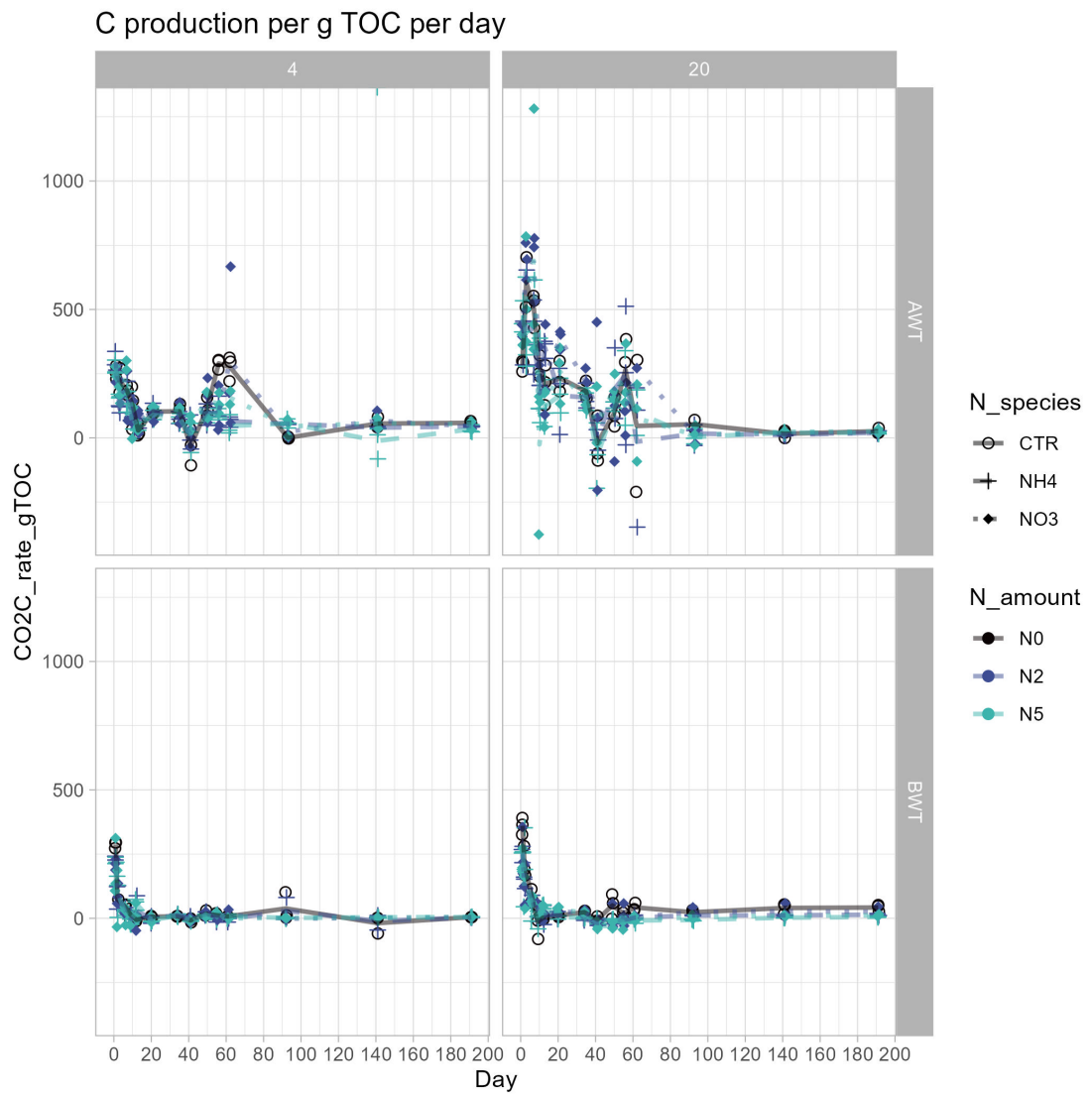
The sample first passes through a 30m SH-Rt-Q-Bond column, which is a nonpolar coated fused silica capillary column that separates CO₂ and methane from O₂, N₂ and CO. Then follows a valve (V-2) whose position is switched between the arrival of methane and CO₂. Its first position directs the flow through a 30m molsieve column (SH-RT-Msieve 5A) that traps moisture and CO and ensures a good peak shape for methane. In the second position, the gas flows through another 30m Q-Bond column that slows the carbon dioxide down. Both pathes then converge on a thermal conductivity detector; this is a nondestructive detector that helps with timing the valve V-2 accurately to retention times of CO₂ and CH₄. Finally the gas flows through an flame ionization detector (FID) equipped with a Jetanizer, a catalyst that turns CO and CO₂ into CH₄ which can be detected by FID.

A.2 Production time series

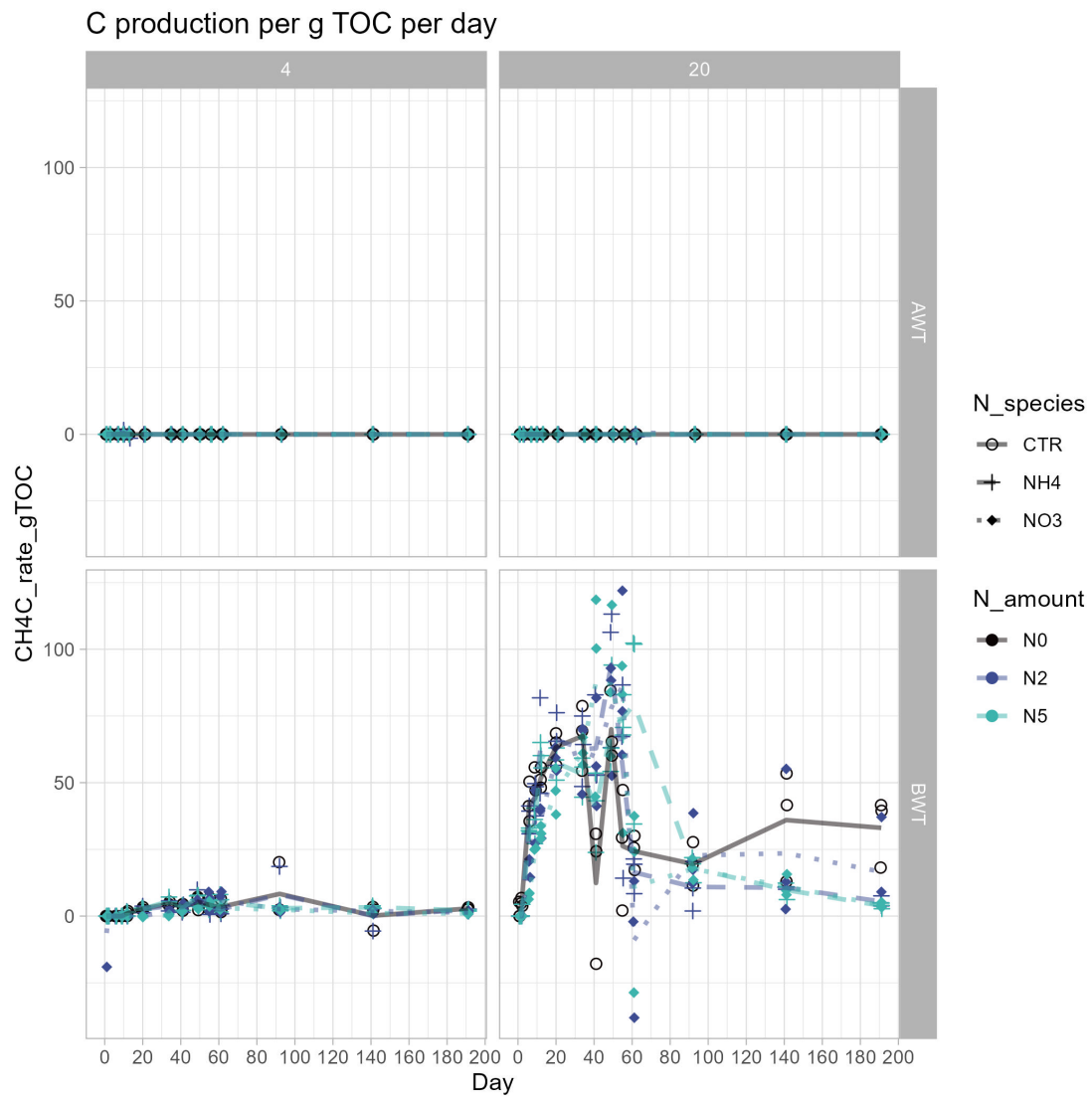
A.2.1 carbon dioxide concentration in blanks



A.2.2 CO₂-C per g TOC per day



A.2.3 CH₄-C per g TOC per day



A.3 multiple linear models

As all models used log-transformed responses, the reported coefficient estimates are backtransformed using $\exp()$ here.

A.3.1 cumulative CO2-C

AWT

N load Residual standard error: 0.2855 on 27 degrees of freedom Multiple R-squared: 0.1166, Adjusted R-squared: 0.0512 F-statistic: 1.782 on 2 and 27 DF, p-value: 0.1875

term	estimate	std.error	statistic	p.value
(Intercept)	10700.00	0.10900	85.400	2.14e-34
total_N_ug	1.00	0.00513	0.893	3.80e-01
temp20	1.19	0.10400	1.660	1.08e-01

N load + form Residual standard error: 0.2265 on 26 degrees of freedom Multiple R-squared: 0.4646, Adjusted R-squared: 0.4028 F-statistic: 7.521 on 3 and 26 DF, p-value: 0.0008804

term	estimate	std.error	statistic	p.value
(Intercept)	1.39e+04	0.10600	89.600	6.40e-34
NH4_N_amount	9.52e-01	0.01360	-3.590	1.34e-03
NO3_N_amount	9.99e-01	0.00424	-0.126	9.01e-01
temp20	1.19e+00	0.08270	2.100	4.59e-02

BWT

N load Residual standard error: 0.6463 on 27 degrees of freedom Multiple R-squared: 0.2948, Adjusted R-squared: 0.2426 F-statistic: 5.644 on 2 and 27 DF, p-value: 0.008957

term	estimate	std.error	statistic	p.value
(Intercept)	1390.000	0.2460	29.40	4.70e-22
total_N_ug	0.983	0.0116	-1.44	1.62e-01
temp20	2.050	0.2360	3.04	5.25e-03

N load + form Residual standard error: 0.5225 on 26 degrees of freedom Multiple R-squared: 0.5562, Adjusted R-squared: 0.505 F-statistic: 10.86 on 3 and 26 DF, p-value: 8.305e-05

term	estimate	std.error	statistic	p.value
(Intercept)	2450.000	0.24600	31.80	2.46e-22
NH4_N_amount	0.875	0.03140	-4.26	2.34e-04
NO3_N_amount	0.973	0.00979	-2.84	8.57e-03
temp20	2.050	0.19100	3.76	8.78e-04

A.3.2 cumulative CH4-C

N load Residual standard error: 0.2825 on 27 degrees of freedom Multiple R-squared: 0.9548, Adjusted R-squared: 0.9514 F-statistic: 284.9 on 2 and 27 DF, p-value: < 2.2e-16

term	estimate	std.error	statistic	p.value
(Intercept)	602.000	0.10800	59.50	3.52e-30
total_N_ug	0.981	0.00508	-3.72	9.18e-04
temp20	11.400	0.10300	23.60	1.51e-19

N load + form Residual standard error: 0.288 on 26 degrees of freedom Multiple R-squared: 0.9547, Adjusted R-squared: 0.9495 F-statistic: 182.8 on 3 and 26 DF, p-value: < 2.2e-16

term	estimate	std.error	statistic	p.value
(Intercept)	603.000	0.1350	47.30	9.56e-27
NH4_N_amount	0.981	0.0173	-1.11	2.76e-01
NO3_N_amount	0.981	0.0054	-3.50	1.69e-03
temp20	11.400	0.1050	23.10	7.20e-19

A.3.3 day of peak CO₂

(not log transformed!)

N load Residual standard error: 14.33 on 55 degrees of freedom Multiple R-squared: 0.238, Adjusted R-squared: 0.1826 F-statistic: 4.294 on 4 and 55 DF, p-value: 0.004282

term	estimate	std.error	statistic	p.value
(Intercept)	24.600	5.130	4.80	1.24e-05
total_N_ug	-0.618	0.257	-2.40	1.98e-02
layerBWT	-21.300	6.770	-3.15	2.65e-03
temp20	-4.670	3.700	-1.26	2.13e-01
total_N_ug:layerBWT	0.624	0.364	1.71	9.23e-02

AWT

N load + form Residual standard error: 18.69 on 26 degrees of freedom Multiple R-squared: 0.2908, Adjusted R-squared: 0.209 F-statistic: 3.554 on 3 and 26 DF, p-value: 0.028

term	estimate	std.error	statistic	p.value
(Intercept)	39.000	8.78	4.44	0.000148
temp20	-9.400	6.82	-1.38	0.180000
NH4_N_amount	-3.100	1.12	-2.76	0.010400
NO3_N_amount	-0.853	0.35	-2.44	0.021900

BWT

N load + form Residual standard error: 0.3121 on 26 degrees of freedom Multiple R-squared: 0.06173, Adjusted R-squared: -0.04653 F-statistic: 0.5702 on 3 and 26 DF, p-value: 0.6396

term	estimate	std.error	statistic	p.value
(Intercept)	0.93200	0.14700	6.350	9.93e-07
temp20	0.06670	0.11400	0.585	5.64e-01
NH4_N_amount	0.01450	0.01880	0.774	4.46e-01
NO3_N_amount	0.00679	0.00585	1.160	2.56e-01

A.3.4 day of peak CH₄

N load Residual standard error: 16.18 on 27 degrees of freedom Multiple R-squared: 0.1421, Adjusted R-squared: 0.07851 F-statistic: 2.235 on 2 and 27 DF, p-value: 0.1264

term	estimate	std.error	statistic	p.value
(Intercept)	52.100	6.160	8.460	4.47e-09
total_N_ug	0.258	0.291	0.889	3.82e-01
temp20	-11.300	5.910	-1.920	6.57e-02

N load + form Residual standard error: 16.1 on 26 degrees of freedom Multiple R-squared: 0.182, Adjusted R-squared: 0.08757 F-statistic: 1.928 on 3 and 26 DF, p-value: 0.1499

term	estimate	std.error	statistic	p.value
(Intercept)	47.100	7.570	6.22	1.39e-06
temp20	-11.300	5.880	-1.93	6.49e-02
NH4_N_amount	1.300	0.968	1.34	1.92e-01
NO3_N_amount	0.357	0.302	1.18	2.47e-01

A.3.5 Q10

CO₂

Residual standard error: 0.5848 on 86 degrees of freedom Multiple R-squared: 0.3648, Adjusted R-squared: 0.3426 F-statistic: 16.46 on 3 and 86 DF, p-value: 1.542e-08

term	estimate	std.error	statistic	p.value
(Intercept)	2.150	0.15900	4.83	5.82e-06
NH4_N_amount	0.896	0.02030	-5.43	5.15e-07
NO3_N_amount	0.984	0.00632	-2.48	1.50e-02
layerBWT	1.720	0.12300	4.41	3.01e-05

CH₄

Residual standard error: 0.3174 on 42 degrees of freedom Multiple R-squared: 0.4936, Adjusted R-squared: 0.4694 F-statistic: 20.47 on 2 and 42 DF, p-value: 6.24e-07

term	estimate	std.error	statistic	p.value
(Intercept)	11.200	0.11200	21.50	2.60e-24
NH4_N_amount	0.956	0.01560	-2.86	6.58e-03
NO3_N_amount	1.020	0.00485	3.12	3.24e-03

A.3.6 released % g TOC

N load Residual standard error: 0.3105 on 55 degrees of freedom Multiple R-squared: 0.8944, Adjusted R-squared: 0.8868 F-statistic: 116.5 on 4 and 55 DF, p-value: < 2.2e-16

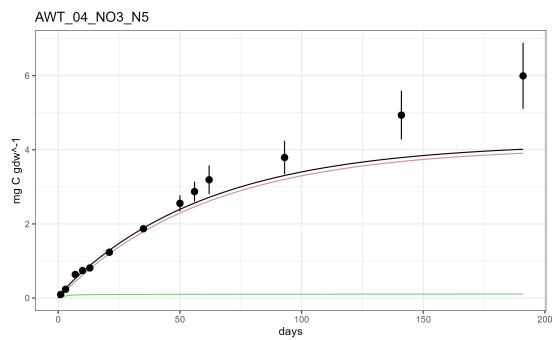
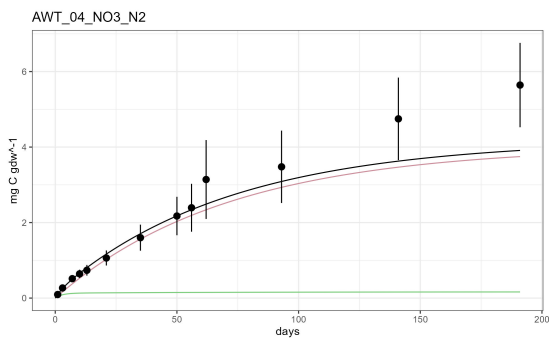
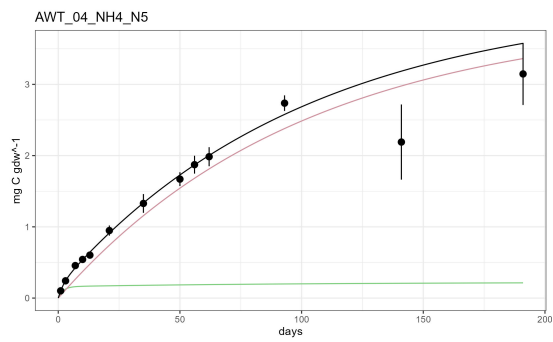
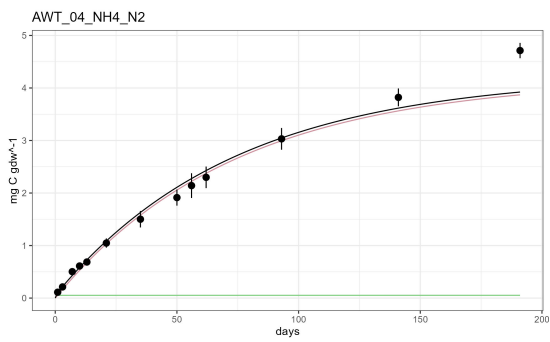
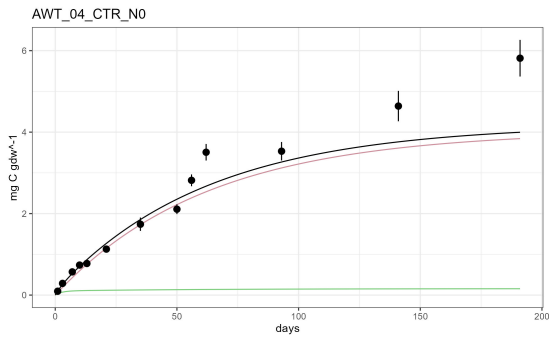
term	estimate	std.error	statistic	p.value
(Intercept)	1.260	0.10100	2.25	2.82e-02
temp20	1.190	0.11300	1.53	1.32e-01
layerBWT	0.134	0.11300	-17.70	2.01e-24
total_N_ug	0.995	0.00394	-1.38	1.74e-01
temp20:layerBWT	4.190	0.16000	8.93	2.70e-12

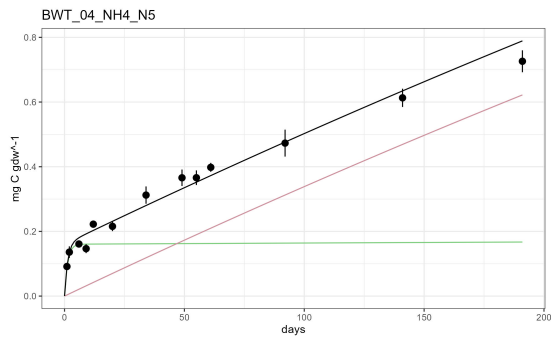
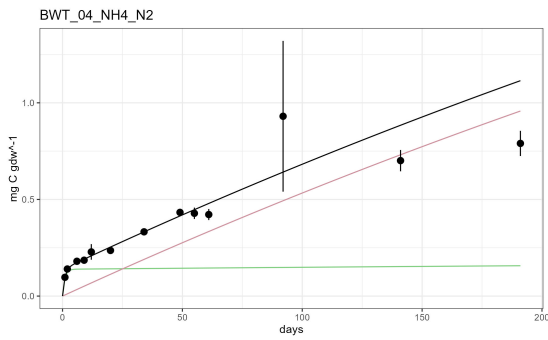
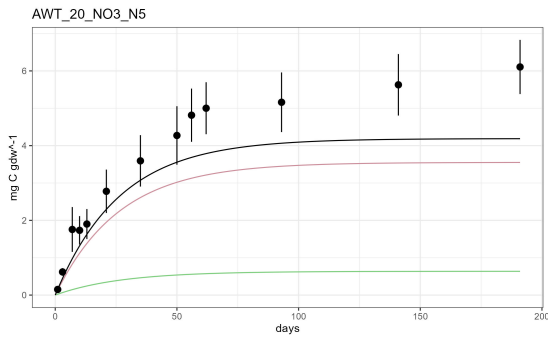
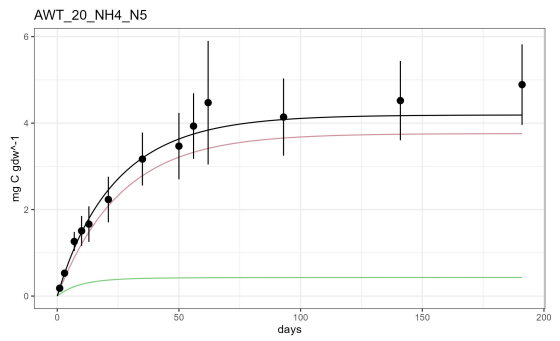
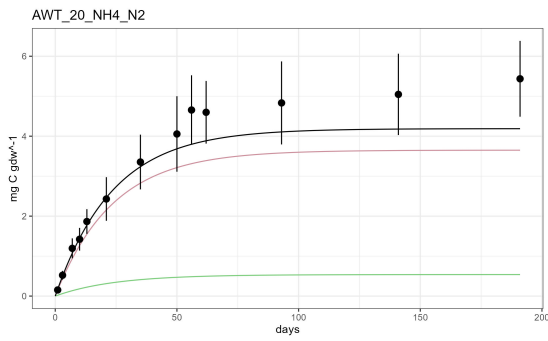
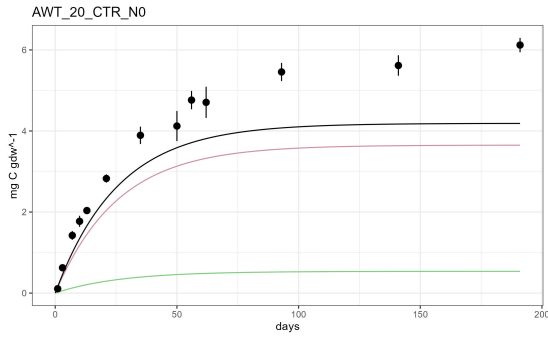
N load + form Residual standard error: 0.2732 on 54 degrees of freedom Multiple R-squared: 0.9197, Adjusted R-squared: 0.9123 F-statistic: 123.8 on 5 and 54 DF, p-value: < 2.2e-16

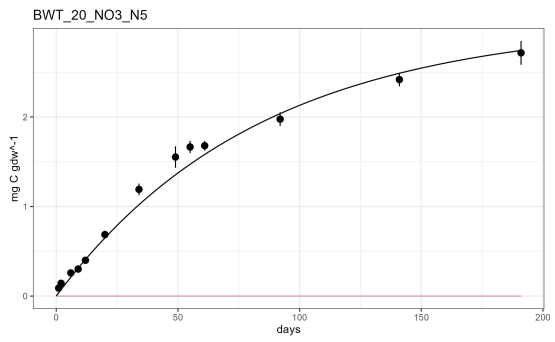
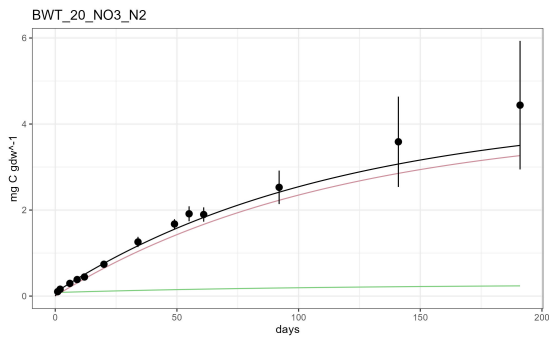
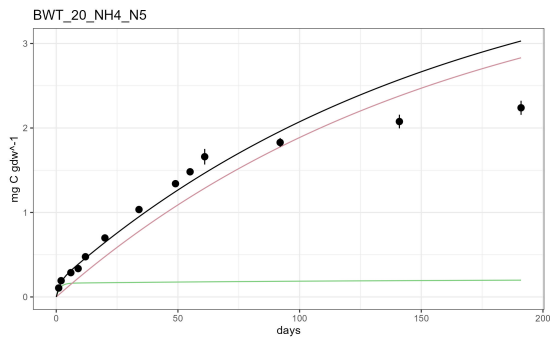
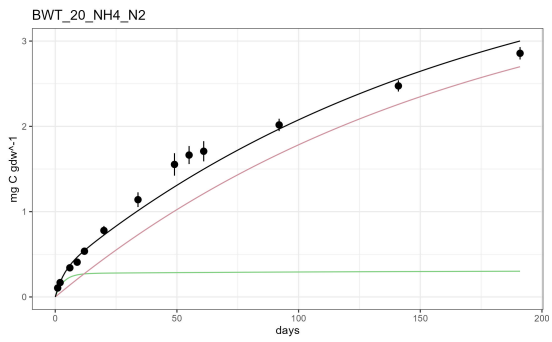
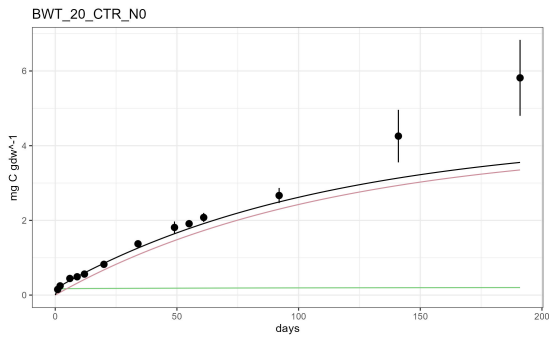
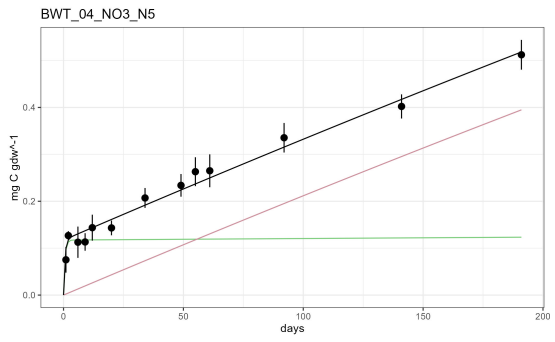
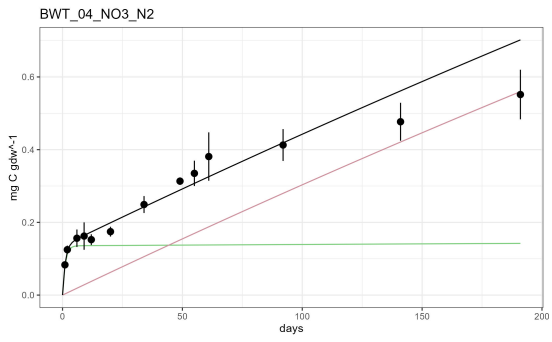
term	estimate	std.error	statistic	p.value
(Intercept)	1.570	0.10400	4.33	6.61e-05
layerBWT	0.134	0.09980	-20.20	8.42e-27
NH4_N_amount	0.950	0.01160	-4.40	5.06e-05
NO3_N_amount	0.990	0.00362	-2.70	9.14e-03
temp20	1.190	0.09980	1.74	8.79e-02
temp20:layerBWT	4.190	0.14100	10.20	4.01e-14

A.4 visualization of fitted decomposition models

Graphs show the cumulative release of carbon as mg C gdw^{-1} from measurements (means \pm standard error of three replicates as points with errorbars), the modelled output (black line) and contributions from pool 1 (green line) and pool 2 (pink line).







A.5 nutrients in tap water and bog

compound	bog background value	addenda (tap water)	addenda (treatments)	measured (extracted water)
Chloride (Cl)	14.42 (8.24) ug/g	65 mg/l	1:1 with NH ₄	
Sodium (Na)		46 mg/l	1:1 with NO ₃	
Calcium (Ca)		100 mg/l		
Sulfate (SO ₄ ²⁻)	10.95 (6.30) ug/g	75 mg/l		
HCO ₃ ⁻	presumably very low	229 mg/l		
Phosphate (PO ₄ ³⁻)	2.12 (3.32)	<0.3 mg/l		
TOC		1,7 mg C/l		42-43%
Nitrate	2.04 (2.75) ug/g	1.0 mg/l	18.4 - 197 mg/l (target: 0.3 - 1.8 mg/l N)	
Nitrite		< 0.03 mg/l		
Ammonium	19.10 (13.77) ug/g	<0.200 mg/l	3.56 - 38.3 mg/l (target: 0.09 - 0.6 mg/l N)	
TIN				
TDN		1 - 1.23 mg/l (sum of iN values)	0.49 - 2.97 mg/l (target concentrations)	3.28 - 23.8 mg/l
TN	0.78 (0.4)%			0.628 - 0.785 % dw (incl. TDN)
pH		7-8		4.0
Fe ₃ ⁺	1.30 (2.43) ug/g	<0,01 - 0,02 (iron in general)		
Mg		46 mg/l		

Table A.1: Background value from H. Zhang et al. (2021), tap water from (Energie und Wasser Potsdam GmbH, 2022)

